PHILOSOPHICAL TRANSACTIONS OF THE ROYAL SOCIETY A MATHEMATICAL, PHYSICAL & ENGINEERING SCIENCES

Transient Phenomena and Impurity Relocation in SIMS Depth Profiling using Oxygen Bombardment: Pursuing the Physics to Interpret the Data [and Discussion]

K. Wittmaack and I. W. Drummond

Phil. Trans. R. Soc. Lond. A 1996 **354**, 2731-2764
doi: 10.1098/rsta.1996.0126

Transient phenomena and impurity relocation in SIMS depth profiling using oxygen bombardment: pursuing the physics to interpret the data

By K. Wittmaack

GSF—National Research Centre for Environment and Health, Institute of Radiation Protection, D-85764 Neuherberg, Germany

High detection sensitivity in bulk analysis or depth profiling by secondary ion mass spectrometry (SIMS) can only be achieved, for positively charged ions, if the near-surface regions of the sputter eroded sample are fully oxidized. Using oxygen primary ions, a stationary oxidation state is established after some time of bombardment during which period the sputtering yield decreases and the ionization probability increases. The physical and chemical processes occurring during the transient period are reviewed with emphasis on the results for impurity analysis in silicon, i.e. the matrix material that has been studied most thoroughly in the past. The transient decrease in sputtering yield gives rise to a depth scale offset and an associated apparent shift of impurity profiles towards the surface. The effect is largest at normal beam incidence, *ca.* 1 nm/keV(O_2^+), in which case silicon is fully oxidized. The transition depth, i.e. the depth sputtered before achieving a stable ion yield is about twice as large and increases as the impact angle is turned away from normal. The shift and the depth scale offset can be measured safely using thin (delta) layers of isotopically pure tracers, for example ^{30}Si in ^{28}Si. Boron delta layers can serve as secondary standards because this impurity behaves almost the same as the host silicon atoms. The profile shift observed with other common dopants may contain contributions due to unidirectional relocation, often driven by segregation away from the surface. At O_2^+ energies below about 0.7 keV the transition depths fall below the thickness of typical native oxides, so that the transient changes in sputtering yield and ionization probability can disappear. The transient phenomena may be described by a simple sputtering–oxidation model that connects the depth scale offset to other observable parameters like the initial and final sputtering yield, the transition fluence and the oxide thickness.

1. Introduction

Over the past 20 years secondary ion mass spectrometry (SIMS) has been used quite successfully for depth profiling impurity distributions in solids. Most of the previous work has been done on semiconductor samples which constitute the major challenge to the SIMS technique because of the need for high sensitivity in combination with high precision (Wilson *et al.* 1989). The excellent sensitivity reported for many elements is based on two characteristic features of SIMS: first, the absence of an inherent

Phil. Trans. R. Soc. Lond. A (1996) **354**, 2731–2764
Printed in Great Britain

background in the secondary ion mass spectrum and second the ability to perform the analysis in such a way that the ionized fraction of the sputtered particles is high (sometimes greater than 1%). Favourable conditions in terms of ion yields, however, can only be achieved after appropriately modifying the chemical composition of the analysed surface. The common approach is to bombard the sample with 'reactive' primary ions such as oxygen (Andersen 1969) or cesium (Andersen 1970). In fact, the fraction of positively charged ions emitted from oxidized samples may exceed the ion fraction from clean metals by up to four orders of magnitude. Likewise, the negative ion yield enhancement achieved by covering a clean sample with a thin layer of alkali metals (submonolayer thickness) may amount to five orders of magnitude (Yu 1991; Wittmaack 1991).

The problem associated with the use of oxygen or cesium primary ion beams is that enhanced and stable ion yields are observed only after the concentration of the implanted probe ions in or on the analysed sample has reached a stationary level. Calibration of impurity concentrations during the initial process of primary ion implantation is impossible without a detailed understanding of beam induced relocation and secondary ion yield enhancement. Moreover, the sputtering yield may change during the build-up period and accurate depth calibration in the transition region becomes very difficult. The latter effect is not very large using cesium primary ions at energies above 1 keV (Wittmaack 1985). For bombardment at near-normal incidence, however, depth calibration errors on the order of 1 nm per keV have been reported some time ago (Wittmaack & Wach 1981). Many groups have subsequently explored the transient effects under oxygen bombardment (Vandervorst & Shepherd 1985; Vandervorst *et al.* 1985; Clegg 1987; Avau *et al.* 1988; Dowsett *et al.* 1992, 1994), but many of the finer details of the process are not yet clear. Attempts have also been made to describe beam induced oxidation and sputtering yield variations by computer simulations (Vancauwenberghe 1992; Vancauwenberghe *et al.* 1992; Svensson *et al.* 1994; Vandervorst *et al.* 1994) and by a simple analytical model (Wittmaack 1996).

Investigations into the physics and chemistry of transient phenomena are very important not only to achieve a better understanding of the relevant processes but also because future device technology requires quantitative analysis of very shallow impurity distributions, with mean ranges of only a few nanometers. At present, the only technique potentially capable of meeting these needs is SIMS. Hence all efforts made to clarify and remove existing shortcomings of the technique are well motivated.

In this review experimental data and the results of model calculations for the transient phenomena in oxygen bombarded silicon are summarized with the aim of acquiring a reasonably coherent picture of the relevant physical (and chemical) processes. Moreover the question is addressed whether it is possible to optimize the operating parameter (beam energy and impact angle) such that the transition depth and the error in depth calibration become equal to or smaller than the thickness of typical contamination layers or of a native oxide.

2. Outline of the problem

The transient effects observed in depth profiling of silicon under oxygen bombardment may be described with reference to figure 1. Let us assume that we want to use SIMS for measuring a shallow depth distribution of impurities like the one depicted in figure 1*a*. For simplicity we ignore at this point that a native oxide and absorbates

PHILOSOPHICAL TRANSACTIONS OF THE ROYAL SOCIETY A MATHEMATICAL, PHYSICAL & ENGINEERING SCIENCES

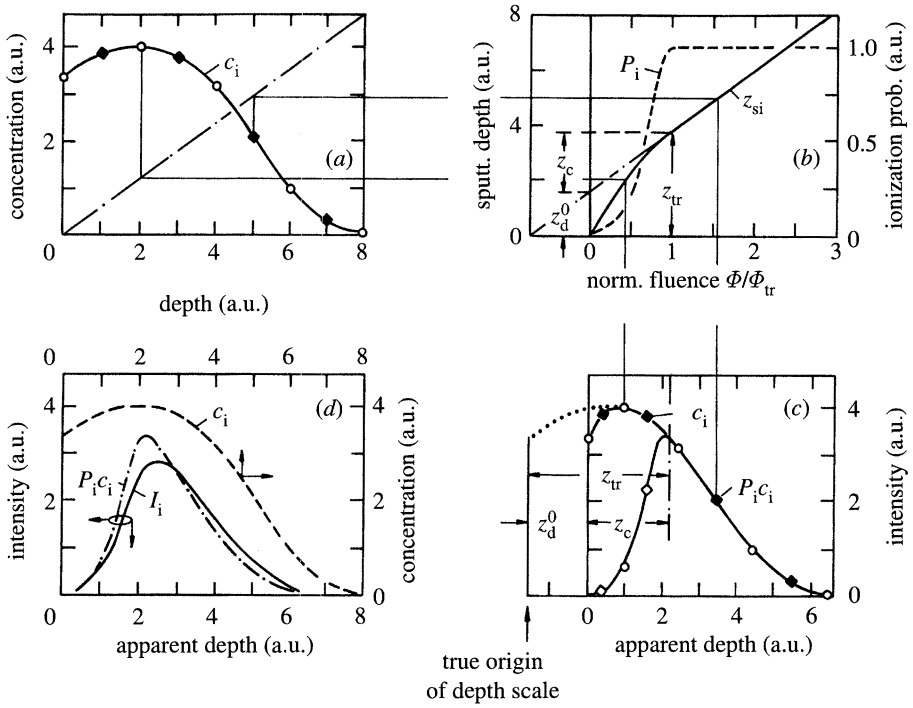

Figure 1. Schematic illustration of transient phenomena in SIMS depth profiling using oxygen bombardment at near-normal beam incidence: (*a*) assumed impurity distribution; (*b*) the depth, z_{Si}, sputtered into silicon and the ionization probability P_i as a function of the normalized bombardment fluence; (*c*) depth profile $P_i c_i$ constructed from (*a*) and (*b*); (*d*) depth profile I_i derived from (*c*) by including bombardment induced mixing.

may be present at the sample surface. To calculate the erosion rate v_{Si} (cm s^{-1}) of the sample as a function of bombardment time t we need to know the silicon sputtering yield $Y \equiv Y_{Si}$, the atomic volume of silicon atoms Ω_{Si} and the primary ion flux ϕ (ions cm^{-2}s^{-1}):

$$v_{Si} = \mathrm{d}z_{Si}/\mathrm{d}t = Y\Omega_{Si}\phi. \tag{2.1}$$

The corresponding volume removal rate ω_{Si} (cm^3 ion^{-1}) is

$$\omega_{Si} = \mathrm{d}z_{Si}/\mathrm{d}\Phi = Y\Omega_{Si}, \tag{2.2}$$

where $\Phi = \phi t$ is the bombardment fluence. If bombardment of the sample is carried out with a raster scanned beam of constant current, the primary ion flux avaraged over many raster cycles will be constant as well. Under these conditions, the silicon erosion rate should also be constant. However, due to the incorporation of primary ions in the sample and their chemical reaction with matrix atoms (oxide formation), an increasing fraction of the beam energy deposited near the surface is being used to sputter previously implanted oxygen. Therefore, the sputtering yield of silicon decreases from Y^0, the number relating to ejection from the virgin sample at the onset of bombardment, to a comparatively low stationary value Y^∞, which represents the partial yield of silicon atoms sputtered from the oxidized sample.

In these general terms the transient changes in sputtering yield are outlined easily. An accurate quantitative description, however, is not yet possible. The reason is that is very difficult to measure the sputtering yield as a function of bombardment fluence.

The most attractive technique for this purpose would be Rutherford backscattering spectrometry (RBS), but only very few data points have been reported up to now for oxygen bombardment of silicon at energies used in SIMS (Dowsett *et al.* 1990; Vandervorst *et al.* 1994). Alternatively one can try to measure sputtering yield changes by surface profilometry, i.e. by determining the depth of the sputtered crater with a stylus technique. The problem is that the enhanced initial silicon removal rate is almost completely compensated by an expansion of the bombarded region due to the incorporation of oxygen (see § 8). In fact, most of the measurements of crater depth z_{cr} versus bombardment time or fluence revealed a linear dependence with an undetectably small zero-fluence offset. In other words, all previous attempts to measure the transient changes in sputtering yield by surface profilometry have failed. This conclusion is based on a recent compilation of literature data (Wittmaack 1996*a*) which revealed very controversial trends and also suggested that the experimental parameters in some of the investigations may not have been well under control.

The lack of success in determining the surface position at low fluences can be understood on the basis of a recent round-robin study (Simons 1996) which showed that the uncertainty δz_{cr} in (careful!) crater depth measurements typically amounts to between 2 and 4 nm for $z_{\mathrm{cr}} \leqslant 100$ nm and 1% for $z_{\mathrm{cr}} > 500$ nm. Since the zero-fluence surface offset z_{s}^{0} has been estimated to 4 nm even at a relatively high O_2^+ probe energy of 10 keV this means $z_{\mathrm{s}}^{0} \lesssim \delta z_{\mathrm{cr}}$, i.e. 'swelling' of the bombarded region due to oxygen incorporation is very hard to detect.

Given this situation, the depth calibration of a raw SIMS profile, i.e. the conversion of the secondary ion intensity or count rate $I(t)$, recorded as a function of time, to the corresponding profile $I(z_{\mathrm{Si}})$, plotted as a function of depth, is commonly achieved by assuming that the silicon erosion rate was constant throughout the whole experiment and equal to the rate determined from the total (final) sputtering time t_{cr} and the crater z_{cr} depth measured *ex situ* after the analysis:

$$v_{\mathrm{Si}} = z_{\mathrm{cr}}/t_{\mathrm{cr}}. \tag{2.3}$$

In reality, however, the silicon thickness z_{Si} eroded as a function of the bombardment time or fluence initially increases nonlinearly. An example resembling oxygen bombardment at near-normal beam incidence is sketched in figure 1*b*. The characteristic fluence required to achieve a constant silicon removal rate is termed the transition fluence Φ_{tr}. The *apparent* thickness eroded at this point is z_{c}, but in reality a much larger amount of silicon, eqivalent to a thickness z_{tr}, has been removed.

The other severe calibration problem associated with the initial oxygen incorporation in the sample relates to the fact that in the fluence range $\Phi \leqslant \Phi_{\mathrm{tr}}$ the ionization probability P_{i} of sputtered atoms and molecules increases strongly, notably for the positive secondary ion species (Wittmaack 1981). These changes are schematically illustrated by the dashed curve in figure 1*b*. We assume that P_{i} becomes constant at the same point as Y, i.e. at $\Phi/\Phi_{\mathrm{tr}} = 1$.

Owing to the fact that a large part of the shallow impurity distribution in figure 1*a* happens to be located in the region $z < z_{\mathrm{tr}}$, the transient changes in sputtering yield and ionization probability will produce a SIMS profile that is strongly distorted (see figure 1*c*). The profile has been constructed point by point from figures 1*a*, *b*, as illustrated schematically by the two thin horizontal and vertical lines connecting identical points on the original and the measured profile. As a natural consequence of the incorrect depth calibration in the near-surface region the whole depth profile originally located beyond z_{tr} appears to be shifted towards the surface by the amount z_{d}^{0}, see figure 1*c*.

It should be noted that any alteration of the original impurity distribution caused by beam induced relocation (mixing) of target atoms is not taken account in the simple picture of figure 1*c*. If mixing is included one has to expect that each 'point' on the original distribution will contribute intensity to the measured profile over a finite range of Φ. The combined action of the three adverse processes, the depth scale offset, the strongly changing ionization probability and the relocation of impurities give rise to an apparent profile (solid line in figure 1*d*) which does not resemble any details of the original distribution (dashed curve). The only safe statement one can make is that a certain amount of impurities must have been present originally at a shallow depth.

Admittedly, the assumed situation constitutes an extreme case, but heavily distorted profiles of this kind have been observed in SIMS measurements, as will be shown in § 4. The ultimate goal must be to avoid or at least to minimize the distortions. In order to find the best compromise it is necessary to understand the correlation between oxygen incorporation and the resulting changes in sputtering yield and ionization probability.

3. Definition and determination of the characteristic shift and broadening parameters

With reference to figures 1*b*, *c* we note that the three characteristic transition and shift parameters z_{d}^0, z_{c} and z_{tr} are related to each other by

$$z_{\mathrm{tr}} = z_{\mathrm{d}}^0 + z_{\mathrm{c}}. \tag{3.1}$$

Considering the complex process of beam induced impurity relocation it is clear that neither the depth scale offset z_{d}^0 nor the transient depth z_{tr} can be derived directly from a SIMS profile. Even a determination of the apparent transition depth z_{c} is only possible if we rely on the assumption that the fluence Φ_{tr} at which, by definition, the sputtering yield becomes constant, is the same as the fluence at which the ionization probability reaches saturation. Assuming $\Omega_{\mathrm{Si}} = \text{const.}$, integration of (2.2) yields

$$z_{\mathrm{c}} = z_{\mathrm{c}}(Y^\infty) \equiv Y^\infty \int_0^{\Phi_{\mathrm{tr}}} \Omega_{\mathrm{Si}}\, \mathrm{d}\Phi = Y^\infty \Omega_{\mathrm{Si}} \Phi_{\mathrm{tr}}. \tag{3.2\,a}$$

To calculate z_{c} from (3.2 *a*), Y^∞ must be known. Φ_{tr} can be determined (*in situ*) from the bombardment parameters and the transition time t_{tr}. Alternatively, using the mean erosion rate derived from an individual (*ex situ*) crater depth measurement,

$$z_{\mathrm{c}} = z_{\mathrm{c}}(\nu_{\mathrm{Si}}) \equiv (t_{\mathrm{tr}}/t_{\mathrm{cr}}) z_{\mathrm{cr}}. \tag{3.2\,b}$$

Using (3.2 *b*), z_{c} can be calculated without an explicit knowledge of the sputtering yield and the transition fluence.

Several examples of matrix ion yield changes observed during the intial stages of silicon bombardment with normally incident oxygen are depicted in figure 2. Also shown are the yields of reemitted O^+ and O_2^+ ions. The apparent depth scales were derived on the basis of (3.2 *a*). During oxygen incorporation all signals in the secondary ion mass spectrum change. However, as figure 2*a* shows (Wittmaack 1987, unpublished results), the different ion species that one can use to monitor the build-up of oxygen exhibit quite different yield variations as a function of bombardment fluence or apparent depth. Consider, for example, the two species Si^+ (dashed line)

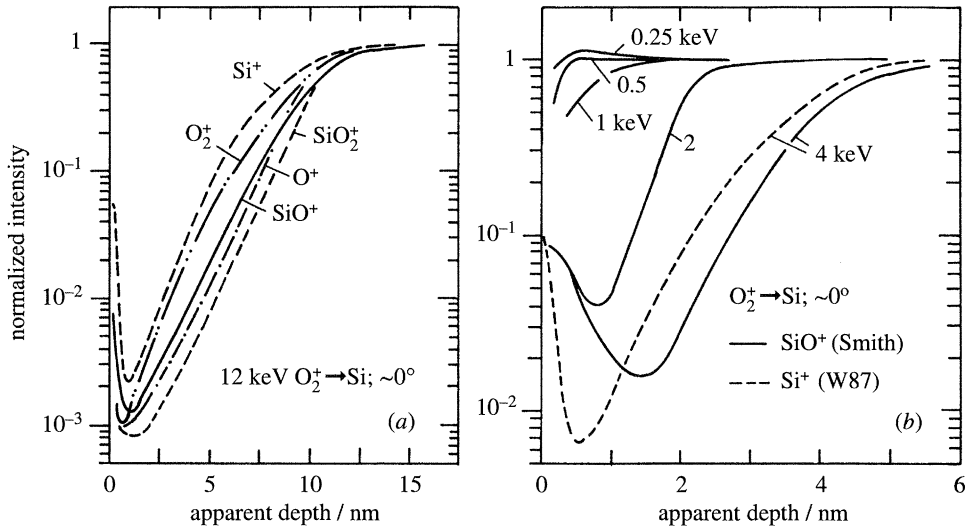

Figure 2. Transient behaviour of various normalized secondary ion signals recorded during the initial period of silicon bombardment with oxygen ions at normal incidence. The data in (*a*) and the dashed curve in (*b*) relate to a sample that had been etched before introduction into the sample chamber (Wittmaack 1987, unpublished results). The solid curves in (*b*) show the effect of beam energy for a sample with a relatively thick native oxide (Smith 1996).

and SiO^+ (full line), which are often used to monitor initial ion yield changes. At the beginning of bombardment these signals are relatively high due to sputtering through the native oxide (which was comparatively thin because the sample had been etched in buffered HF prior to being inserted into the sample chamber). By the time most of the surface oxide has been removed the signals pass through a minimum, then start to increase rapidly because the oxygen concentration at the surface builds up continuously. Finally the signals arrive at a stationary level. A detailed discussion of the differences in ion yield evolution is beyond the scope of this paper. The important message of figure 2*a* is that the *apparent* depth which needs to be sputtered in order to reach more than 90% of the stationary level is the same for the different species to within ±8%. Within this uncertainty any of the species monitored in the experiment of figure 2*a* may serve to determine the apparent transition depth for 12 keV O_2^+ incident on Si at 0°. We find $z_c = (12.5 \pm 1)$ nm.

The effect of ion energy on the transient changes of the SiO^+ yields is illustrated in figure 2*b* by the solid lines (Smith 1996). This sample contained a top layer grown by ion beam deposition of isotopically pure Si beams. By the time of the depth profiling experiment the sample was about five years old (Dowsett 1996, personal communication). In qualitative terms the yield curves observed using 2 or 4 keV O_2^+ ions are similar to those at 12 keV (figure 2*a*). However, the minima are considerably less deep and the surface oxide appears to be comparatively thick. This supposition is supported by the dashed curve in figure 2*b* which shows data for 4 keV O_2^+ obtained on the same sample as the one used to collect the data in figure 2*a* (Wittmaack 1987, unpublished results). The near-surface signal fall-off proceeds much faster for the dashed than for the continuous curve. Moreover, at the same beam energy, the spacing between the minima for 4 keV amounts to about 1 nm, a number that could be interpreted as a rough measure of the difference in surface oxide thickness.

The indirect evidence for the presence of a relatively thick native oxide on the

sample(s) used by Smith (1996) appears to be important for an understanding of the rather abrupt change in the shape of the build-up curves that was observed upon lowering the beam energy from 2 to 1 keV and less (figure 2*b*). At the lowest beam energies the transient variations in secondary ion yield are reduced to a factor of two or less. Under these conditions the thickness of the native oxide was approximately commensurate with the width of the transition layer. A more detailed discussion of this aspect will be given in § 8.

Once the apparent transition depth z_c has been derived according to the procedure outlined in figure 2, the next step is a determination of the depth scale offset z_d^0. Clearly, this number cannot be evaluated using shallow impurity distributions like the one sketched in figure 1*a*. In order to avoid all problems associated with the initial changes in ionization probability one should use buried tracer distributions located at a depth $z_0 > z_{tr}$. However, even when using such dedicated samples we are facing the question whether and how the original tracer location can be retrieved from the measured profile. This issue may be discussed with reference to results of analytical calculations and computer simulations on beam induced broadening in sputter profiling of thin tracer layers. In the models the sputtering yield and the erosion velocity were considered constant, i.e. there was no profile shift due to an initial decrease in sputtering yield. In the most simplified approach to the problem sputter profiles have been calculated on the basis of a diffusion approximation. Under the assumption that the depth of origin, z_{or}, of the sputtered atoms is zero and the ejection probabilities of tracer and host atoms are the same (no preferential sputtering), moments of the profile of the tracer concentration at the receding surface and of the decay length could be determined analytically (Naundorf & Abromeit 1989). It turned out that the first moment of the profile, i.e. the mean depth or centroid $\langle z \rangle$, is equal to z_0, the original tracer location, $\langle z \rangle = z_0$.

If the depth of origin is not negligibly small, $z_{or} > 0$, this has the effect of shifting the sputter profile towards the surface by about the same amount (shifts different from z_{or} may be expected if pronounced concentration gradients are established in the outermost layers of the receding surface). The aspect has been explored by computer simulations based on a transport theory of recoil mixing (Littmark & Hofer 1984). The tracer was assumed to be 1 nm thick and centred at a sufficiently large depth z_0 (see figure 3*a*), so that in course of sputter profiling by 2 keV Ne the complete damage distribution was passing through the tracer. The spacing between the profiles of the sputtered flux (full line) and the surface concentration (dashed line) amounts to about 0.6 nm, essentially the same number as the mean depth of origin inherent in the simulation code (Littmark & Hofer 1980).

The effect of the relative escape probability (or preferential sputtering factor) r on the shape and location of surface concentration profiles is shown in figure 3*b* for three values of r. The profiles were calculated using the diffusion approach (King & Tsong 1984). Depending on whether the tracer atoms are assumed to be sputter ejected with enhanced or reduced efficiency relative the matrix atoms, i.e. $r > 1$ or $r < 1$, the peaks are higher (lower) and appear at smaller (larger) depth than the reference profile, $r = 1$. As r is varied from 0.56 to 1.8 the peak shifts towards the surface by 1.2 nm.

In addition to, or as an alternative to, $\hat{z}$ and $\langle z \rangle$, the median depth z_{md} can serve for describing the profile location. The latter number, which defines the depth at which 50% of the atoms originally contained in the delta distribution have been sputtered, may be determined by counting the area under the profiles in figure 3*b*.

PHILOSOPHICAL TRANSACTIONS OF THE ROYAL SOCIETY A MATHEMATICAL, PHYSICAL & ENGINEERING SCIENCES

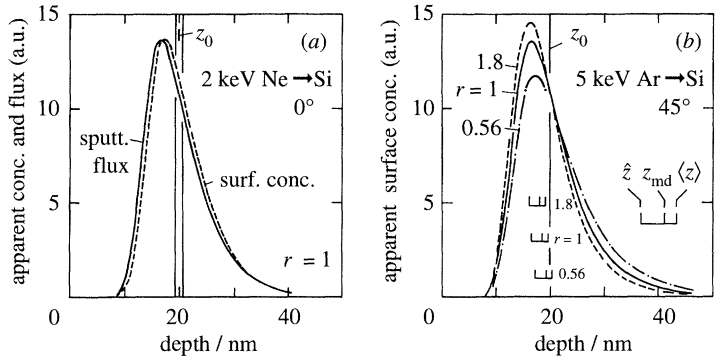

Figure 3. Calculated depth profiles for (*a*) a thin layer and (*b*) a delta layer of Si in Si. The results in (*a*) show the difference between the sputtered flux and the surface concentration caused by a non-vanishing depth of origin of sputtered atoms (Littmark & Hofer 1984). The curves in (*b*) illustrate the effect of the escape probabilty r (King & Tsong 1984).

As in range caculations (Winterbon 1975) one can use approximate formulas of the theory of statistics to correlate the mean, the mode and the median of a profile:

$$3z_{\mathrm{md}} - 2\langle z\rangle - \hat{z} = 0. \tag{3.3}$$

For profiles skewed towards the surface, (3.3) implies $\hat{z} < z_{\mathrm{md}} < \langle z\rangle$. The three different profile parameters are marked in figure 3*b* by vertical bars. Within the accuracy of profile evaluation, $\langle z\rangle \approx z_0$ for $r = 1$, in agreement with the analytical result obtained from the diffusion approximation of sputter profiling (Naundorf & Abromeit 1989).

We conclude from the results of figure 3 that for mixing in an (isotropic) collision cascade, or by equivalent processes, the mean depth $\langle z\rangle = \langle z\rangle_{\mathrm{is}}$ constitutes the best first-order choice for determining the original tracer location. However, if the finer features of the sputtering process are included, such as $z_{\mathrm{or}} > 0$, then

$$z_0 = \langle z\rangle_{\mathrm{is}} + z_{\mathrm{or}}, \quad \text{for } r = 1. \tag{3.4}$$

If $r \neq 1$, the measured profile position $\langle z\rangle_{\mathrm{is}}$ can deviate from the true tracer location z_0 by more than 1 nm in either direction.

We now turn to a real experiment using oxygen bombardment. Figure 4*a* shows SIMS profiles of a boron delta (B-δ) doping spike grown by molecular beam epitaxy (MBE). The spike was located at a nominal depth of about 22 nm. Accidentally a small amount of boron was incorporated in the substrate just prior to the growth of the spike. This unintentional doping shows up as a shoulder on the large-depth side of the prominent peaks in figure 4*a*. The profiles were obtained using O_2^+ primary ions at two different energies, 1.5 and 4 keV, but with the same angle of beam incidence, $\theta \approx 5°$ to the surface normal (Wittmaack 1996*a*).

Before discussing the measured delta doping profiles we consider the boron signals recorded near the surface, i.e. at apparent depths of less than 10 nm. Apparently the sample was covered with a thin contamination layer containing boron. This kind of contamination has been known for some time (Wach & Wittmaack 1982*a*). Thin impurity or contamination layers at the sample surface constitute very useful tracers (Wittmaack 1987) for measuring the so-called decay length λ_{d} which characterizes the exponential depth dependence of impurity signals observed with narrow doping distributions, irrespective of whether they are located at the surface or somewhere

PHILOSOPHICAL TRANSACTIONS OF THE ROYAL SOCIETY A MATHEMATICAL, PHYSICAL & ENGINEERING SCIENCES

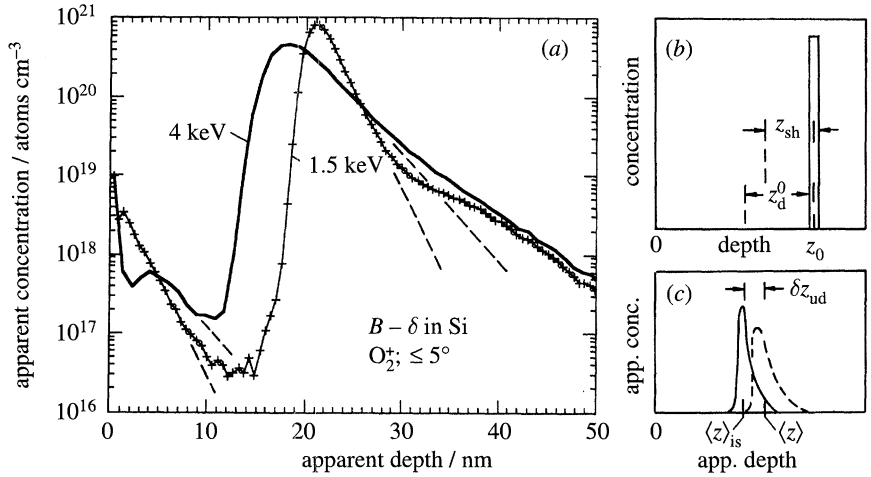

Figure 4. (*a*) Depth profiles of a non-ideal delta layer of boron in silicon measured at two different oxygen energies. The dashed lines show the exponential signal decay expected for an ideal delta layer. (*b*) Schematic drawing of an ideal thin layer. (*c*) Schematic drawing of the SIMS profile measured with a sample as in (*b*), without and with unidirectional relocation, full and dashed curve, respectively. The shift and broadening parameters are explained in the text.

in the bulk of the sample:

$$I(z_{\mathrm{Si}}) \propto \exp(-z_{\mathrm{Si}}/\lambda_{\mathrm{d}}). \tag{3.5}$$

The inverse decay length $\lambda_{\mathrm{d}}^{-1}$ is proportional to the (mean) surface concentration in the internal distribution of intermixed impurities, p_0, as well as to the relative ejection probability r, i.e. $\lambda_{\mathrm{d}}^{-1} = p_0 r$ (Wittmaack 1992). For surface impurities a clear exponential signal fall-off can be expected only at depths $z > z_{\mathrm{tr}}$. In figure 4*a* this kind of behaviour is clearly established for the profile measured with 1.5 keV O_2^+, at apparent depths between 2 and about 8 nm. Owing to the relatively low energy a sizable amount of boron originating from the contamination layer had not yet been sputtered at the apparent transition depth, so that the exponential decay was observable through two orders of magnitude in signal height.

Considering the buried delta distribution we note three important features. (i) Both profiles exhibit steeply rising leading edges and slowly decreasing large-depth tails. (ii) The difference in bombardment induced boadening is relatively small at the leading edge but rather large at the trailing edge (the true exponential tails, significantly masked by the doping shoulder, are indicated by the dashed straight lines). (iii) For each apparent concentration level the relative shift between the two profiles is seen to be different and on the large-depth side of the profiles the shift even changes sign.

With the results of figure 3*a* in mind we may determine the sputter offset z_{d}^0 produced during the initial phase of oxygen implantation from a first-order approach

$$z_{\mathrm{d}}^0 = z_0 - \langle z\rangle_{\mathrm{is}}, \tag{3.6}$$

which implies that the original tracer location z_0 is known from other sources, e.g. from the growth parameters of the sample. It is also assumed that bombardment induced relocation processes are isotropic. In general, however, one has to expect not only a broadening but also a superimposed unidirectional impurity transport which produces an additional contribution, δz_{ud}, to the observed profile shift. Recoil implantation, for example, is a process that gives rise to non-isotropic collisional

relocation. In the special case of oxygen bombardment it is likely that unidirectional transport driven by chemical forces (e.g. segregation) will play a significant, if not dominant role (Wittmaack 1994*a*). On the apparent depth scale the centroid will then be observed at $\langle z \rangle$ and the total shift, z_{sh}, of this feature is the sum of the depth scale offset z_{d}^{0} and the unidirectional shift δz_{ud}:

$$z_{\mathrm{sh}} = z_0 - \langle z \rangle = z_{\mathrm{d}}^{0} + \delta z_{\mathrm{ud}}. \tag{3.7}$$

A schematic illustration is given in figures 4*b*, *c*. Since the apparent and the true shift components, z_{d}^{0} and δz_{ud}, are both counted positive when directed towards the original surface, segregation of impurities away from the receding surface (δz_{ud} negative) has the effect of making z_{sh} smaller than z_{d}^{0}. With certain impurities one may encounter a situation such that the depth scale offset z_{d}^{0} is completely balanced by segregation, i.e. $z_{\mathrm{sh}} = 0$. Examples will be discussed in § 5. In any case, one needs sufficiently accurate information about δz_{ud} if one wants to determine z_{d}^{0} by way of measuring $\langle z \rangle$.

Important insight into the magnitude of bombardment induced impurity relocation may be obtained by comparing transient ion yield changes of impurity and reference species at fluences around Φ_{tr}. Two types of samples can be used, (i) silicon uniformly doped with the impurity under study or (ii) silicon containing the impurity (only) in the form of a thin layer deposited at the surface. A comparison of results for Sb in Si, obtained with such test samples, is presented in figure 5 (Wittmaack 1993). The transient changes in oxygen content of the samples were monitored by recording O_2^+ secondary ions which closely resemble the build-up of Si^+ (see figure 2*a*) (the reason for using O_2^+ ions as reference species was that the Si^+ count rates would have exceeded the limit above which dead time losses of the multiplier become intolerably large, even for $^{30}Si^+$, the silicon isotope of lowest abundance).

With the uniformly doped sample (figure 5*a*), the impurity and the reference signal exhibit very similar changes up to an apparent depth of about 4 nm. Thereafter, the O_2^+ signal continues to increase in the same manner as in figure 2*a* and stabilizes at about 6 nm. The Sb^+ signal, however, passes through a local maximum ('pre-saturation peak' at 4.5 nm) followed by a minimum and then continues to increase to an apparent depth of at least 12 nm. This behaviour implies that in order to produce a stable internal distribution of Sb in the oxygen bombarded sample, it is necessary to sputter to a depth significantly larger than z_{tr}.

It appears from the results of figure 5*a* that the Sb^+ signal approaches the stationary level only exponentially, $I(z_{\mathrm{Si}}) \propto 1 - \exp(-z_{\mathrm{Si}}/\lambda_{\mathrm{d}})$. Since the Sb^+ count rates were relatively low, the finer details of signal evolution at depths exceeding 10 nm are hidden in the counting statistics. An exponential depth dependence of the Sb^+ signal is, however, clearly evident in figure 5*b* which shows results of the 'inverse' experiment, where Sb was present only as a thin surface layer. To get to the point where the fall-off is truly exponential ($\lambda_{\mathrm{d}} = 5.4$ nm) one has to sputter to an apparent depth of about 12 nm, in agreement with the results of figure 5*a*. The local variations in signal around 5 nm are also very similar in the two types of experiments.

We conclude that studies on the transient variation of impurity signals are well suited for deriving information about beam induced transport phenomena. Impurity signals may also be used as secondary standard for determining the apparent and/or the true transition depth, but only if their behaviour is known from a 'calibration' against matrix signals, as shown in figure 5 (Φ_{tr} corresponds to the position of the minimum or edge of the shoulder behind the local Sb^+ peak).

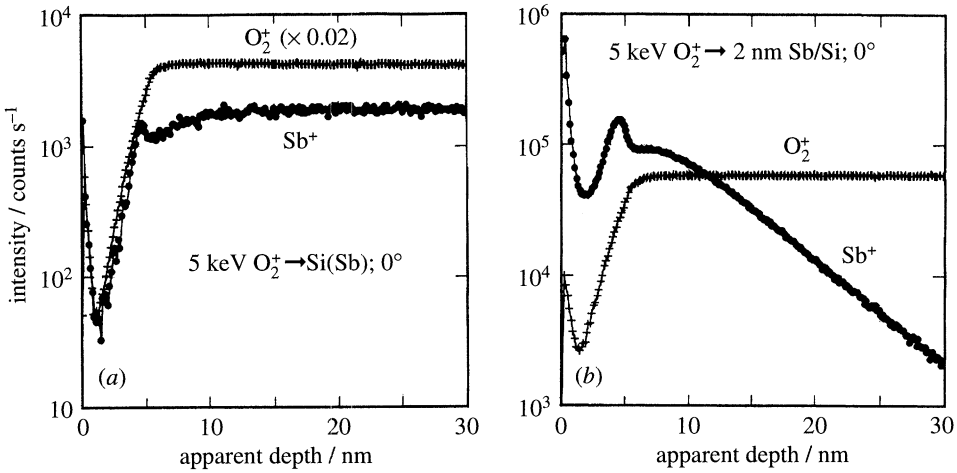

Figure 5. Transient behaviour of Sb^+ and O_2^+ secondary ion signals during the initial period of oxygen bombardment: (*a*) silicon uniformly doped with Sb; (*b*) silicon covered with a thin layer of Sb (Wittmaack 1993).

4. Examples of distorted and corrected impurity profiles

SIMS depth profiles resembling the situation sketched in figure 1 are shown in figure 6*a*. Implantation distributions of 4–25 keV Sb in Si were measured using 12 keV O_2^+ ions at near-normal beam incidence, $\theta = 2°$ (Avau *et al.* 1988). Considering the chosen energies of the implanted ions and the probe ions it is clear that a sizable fraction of the implantation profile will fall into the transient region. In fact, except for a difference in the position of the pre-saturation peak (at an apparent depth of 10 nm), the evolution of the Sb^+ signals relating to implantation energies of 4 and 10 keV is very much the same as for the Sb surface layer in figure 5*b*. The two heavily distorted profiles exhibit exponential tails with the same decay length of (7.5 ± 0.5) nm. In order to observe a reasonably well defined implantation peak under the chosen SIMS depth profiling conditions the implantation energy has to be at least as high as 25 keV (see figure 6*a*). But even for this profile the long range tail is the same as for the low implantation energies, i.e. the tail is determined by beam induced broadening and not representative of the true implantation distribution. Hence, in terms of quantitative analysis, the SIMS profiles for implantation energies below about 20 keV in figure 6*a* are completely useless. They merely contain the information that a certain amount of antimony was originally present in the region between the surface and a depth of about 25 nm (assuming here that $z_{\mathrm{tr}} \approx 2z_{\mathrm{c}}$). This depth happens to be equal to the sum of the projected range and the range straggling, $R_{\mathrm{p}} + \Delta R_{\mathrm{p}}$, of 12 keV O_2^+ (6 keV atom^{-1}) in Si (Wach & Wittmaack 1983; Ziegler *et al.* 1985).

As to be expected, the SIMS profile for a relatively deep implantation distribution, 100 keV Sb in Si (figure 6*b*), exhibits distortions only at a depth which is small compared to the mean range (note the different depth scales in figures 6*a*, *b*). In order to determine z_{sh} according to (3.7) we compare the SIMS profile with accurate range data that have been obtained by high-resolution RBS (Kalbitzer & Oetzmann 1980). From the universal curve for the projected mean range R_{p} of heavy ions in Si we find, for 100 keV Sb in Si, $R_{\mathrm{p}} = (54 \pm 2)$ nm. Since the profile is almost Gaussian, the mean range is only slightly larger than the most probable (modal) range $\hat{R}$. On

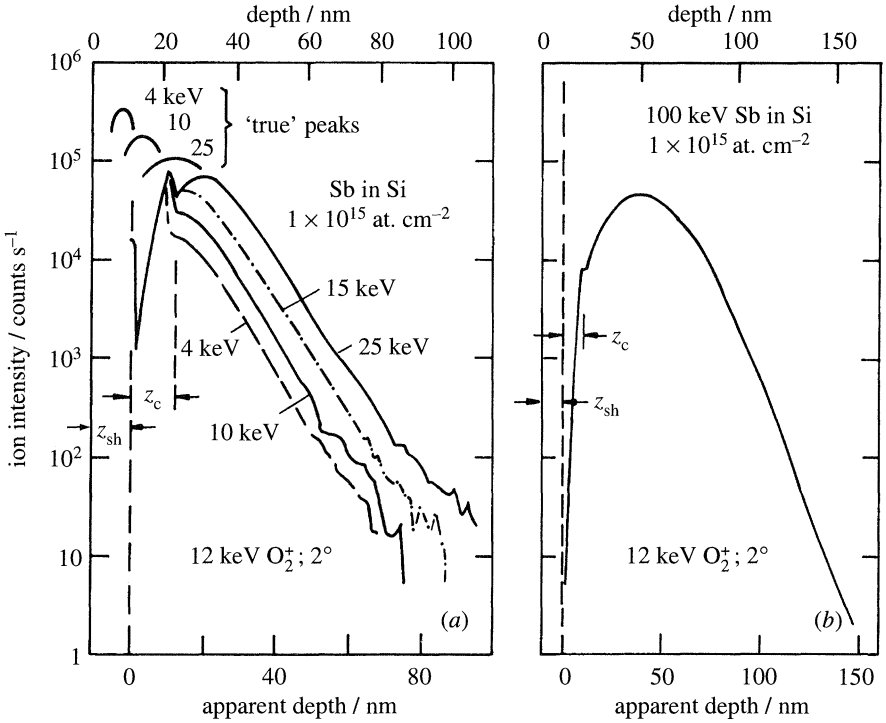

Figure 6. SIMS depth profiles of Sb implanted in Si, measured at a relatively high O_2^+ probe energy of 12 keV: (*a*) low; and (*b*) high implantation energies. The evaluation of the true depth scale at the top is explained in the text. Adapted from Avau *et al.* 1988.

this basis the true depth scale (top scale in figure 6*b*) is obtained by shifting the measured profile to the extent that $\hat{R} \approx (50 \pm 3)$ nm. This procedure yields a profile shift z_{sh} of (11 ± 3) nm.

If we use this number for z_{sh} to correct the depth scale in figure 6*a* we see that, in agreement with the reasoning outlined above, the 4 keV implantation distribution was located almost completely in the transient region. One may construct the peak regions of the 'true' profiles for 4, 10 and 25 keV Sb from the signal height in figure 6*b* and the range data of Kalbitzer & Oetzmann (1980), assuming a constant relative range straggling $\Delta R_p/R_p = 0.38$, and a peak height inversely proportional to ΔR_p. This procedure (figure 6*a*) illustrates the very large amount of bombardment induced distortions produced under the chosen conditions.

It had been shown already in the experiments of Wittmaack & Wach (1981) that the profile shift and the apparent transition depth can be reduced by lowering the probe energy (see also figure 2*b*). Alternatively one can try to reduce the magnitude of the profile shift by bombardment at oblique beam incidence. The argument in favour of ion impact at angles sufficiently away from normal incidence is that only incomplete oxidation is achieved. Hence the changes in sputtering yield during the transient period and the depth scale offset will be smaller than at normal incidence. In accordance with this idea Clegg (1987) reported a five times smaller (differential) shift for B in Si using an impact angle of 45° instead of 2°. Figure 7*a* shows the initial section of a SIMS profile of 25 keV As in Si measured with a 2 keV O_2^+ beam incident at 45°. From the build-up curves for the Si^+ and O^+ signals one derives an apparent transition depth of about 10 nm so that with $z_{sh} \approx 0.5$ nm we have $z_{tr} = 10.5$ nm.

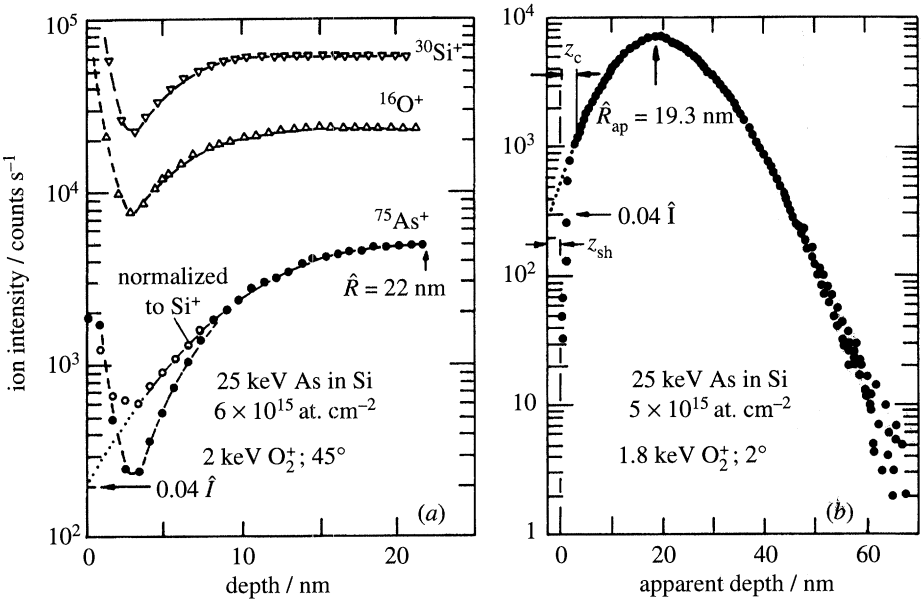

Figure 7. (*a*) Initial section of a SIMS depth profile of As in Si, measured at an oxygen impact angle of 45° (Clegg 1987). (*b*) The same implantation distribution as in (*a*), but measured at near-normal beam incidence (Vandervorst *et al.* 1984).

This is significantly larger than the transition depth of 5.5 nm ($z_c = 2.5$ nm, $z_{sh} = 3$ nm) measured in the same study for near-normal incidence (2°). The results implies that z_{sh} and z_{tr} respond differently to a change in impact angle θ: with increasing θ the shift z_{sh} decreases but z_{tr} increases. This aspect will be discussed in more detail in § 7.

Clegg (1987) has attempted to correct the As^+ yields by normalizing the data to the Si^+ yield. As the oxygen induced ion yield enhancement is relatively small for $\theta = 45°$ the correction procedure may be applicable (but needs independent justification). The corrected profiles derived using ion yield ratios agreed very well for probe energies of 1 and 2 keV.

Arsenic depth profiles measured at near-normal beam incidence have been reported by Vandervorst *et al.* (1984). Figure 7*b* shows an example that relates to the same implantation energy as in figure 7*a*. In accordance with figure 2*b* and with the findings reported by Clegg (1987) the apparent transition depth for normally incident 1.85 keV (*ca.* 2 keV) O_2^+, i.e. the end point of the initial steep signal rise in figure 7*b*, is found to be (2.5 ± 0.5) nm. To get the same modal range as in figure 7*a* ($\hat{R} = 22$ nm) a profile shift of 2.7 nm must be added to the apparent modal range $\hat{R}_{ap} = 19.3$ nm of the profile in figure 7*b*. With that correction the two profiles agree very well, including such finer details as the normalized ion yield $\hat{I}_{sf}/\hat{I}$ at the surface, which turns out to be 0.04 for 25 keV As (see extrapolated dotted curves in figures 7*a*, *b*).

Further inspection of the (corrected) range data for implantation energies between 4 and 100 keV shows very good agreement between the two sets of SIMS data as well with results of high-resolution RBS measurements (Kalbitzer & Oetzmann 1980). Hence, using adequate bombardment conditions, low-energy SIMS is a reliable technique for characterizing shallow doping distributions.

PHILOSOPHICAL TRANSACTIONS OF THE ROYAL SOCIETY A MATHEMATICAL, PHYSICAL & ENGINEERING SCIENCES

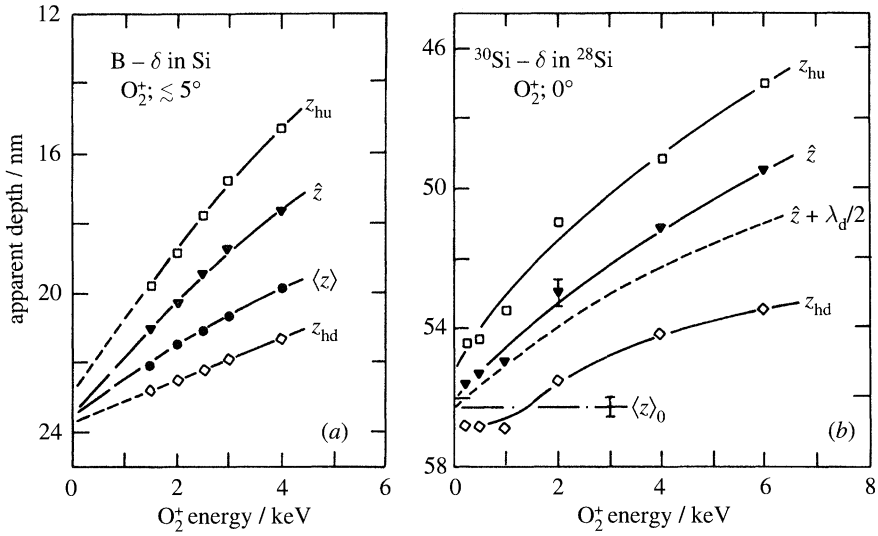

Figure 8. (*a*) Impact-energy dependence of apparent profile parameters of a B-δ distribution in Si, measured by oxygen bombardment at near-normal beam incidence (Wittmaack 1996*a*). (*b*) The same as (*a*), but for a ^{30}Si-δ embedded in matrix of ^{28}Si (from Smith *et al.* 1996). Note that the depth increases from the top to the bottom of the figures.

5. Energy dependence of profile shifts and transition depths

It was already shown in figures 2*b* and 3*a* that the (apparent) transition depth and the profile shift can be reduced by lowering the beam energy. However, in order to determine the shift z_{d}^0 in absolute terms one needs to know the the original tracer location z_0, see (3.7). This number is usually not known with the desired accuracy of ± 0.5 nm. Hence many groups have tried to derive the lacking information by performing depth profiling measurements on delta doping distributions as a function of beam energy (Clegg 1987; Barlow *et al.* 1992; Dowsett *et al.* 1992, 1994; Smith *et al.* 1996; Wittmaack 1996*a*). Figure 8*a* shows shift data derived from SIMS profiles of the boron delta (B-δ) distribution described with reference to figure 2*a* (Wittmaack 1996a). The data are plotted on an inverted depth scale so that the increase in shift with increasing beam energy becomes evident. The apparent positions of the leading (up) and trailing (down) edges at half the apparent peak concentration are labelled z_{hu} and z_{hd}, respectively, the apparent peak positions and the apparent mean locations (centroids) are denoted $\hat{z}$ and $\langle z \rangle$, respectively. The effect of increasing beam energy is seen to be large for z_{hu} but comparatively small for z_{hd}. This observation can be attributed to the well-known fact that beam induced broadening is small at the leading and large at the trailing edge (long trailing edges have the effect of moving z_{hd} away from the surface, thus reducing the apparent shift). Extrapolating the data for z_{hu} and z_{hd} to the limit of vanishing beam energy, $E \rightarrow 0$, yields intercepts on the ordinate that differ by about 1 nm, a number that may be interpreted as the original width of the (non-ideal) delta doping distribution. Moreover we see that the spacing between $\hat{z}$ and $\langle z \rangle$ decreases continuously with decreasing energy, i.e. $\hat{z} \rightarrow \langle z \rangle$ for $E \rightarrow 0$, which is quite reasonable for (symmetric) sufficiently narrow doping distributions.

Depth profiles for a delta doping distribution of ^{30}Si embedded in a matrix of ^{28}Si have recently been reported by Smith *et al.* (1996). From the profiles one can derive

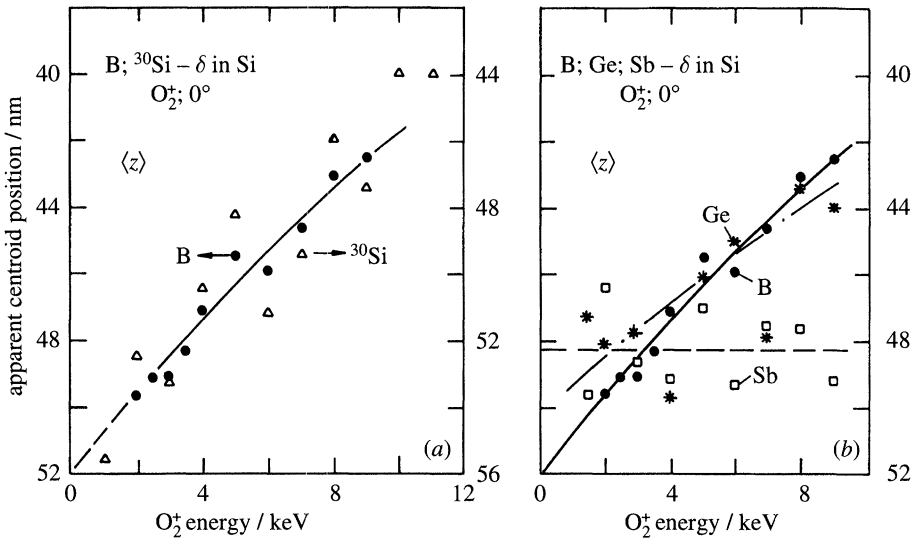

Figure 9. Impact-energy dependence of apparent centroid positions for different delta layers in Si measured by oxygen bombardment at normal incidence: (*a*) B- and ^{30}Si-δs; (*b*) B-, Ge- and Sb-δs. Note that the depth increase from the top to the bottom of the figures (Dowsett *et al.* 1992, 1994).

the energy dependence of $\hat{z}$, z_{hu} and z_{hd} shown in figure 8*b*. The apparent centroid position may be assessed using the approximation, $\langle z\rangle \approx \hat{z} + 0.5\lambda_{\mathrm{d}}$, an empirical relation based on results for B-δs. Extrapolation of the dashed line in figure 8*b* to $E = 0$ suggests that the ^{30}Si-δ was originally located at a depth $z_0 = (56.3 \pm 0.3)$ nm. Within experimental uncertainty the apparent centroid position of the ^{30}Si-δ exhibits the same variation with beam energy as the B-δ in figure 8*a*. Further evidence in this respect is provided by the results of figure 9*a*, which shows a direct comparison of apparent centroid positions for B-δ and Si-δ distributions in Si (Dowsett *et al.* 1994). Although the scatter of the data for the Si-δ is somewhat large, the similarity in the profile shifts measured for the two dopants is evident.

These findings support the idea (Wittmaack 1996*a*) that boron deltas are well suited for determining the depth scale offset z_{d}^0. The argument is as follows. Considering first the Si-δ we note that chemical effects are absent in studies on isotopic tracers buried in a matrix of the same element. Furthermore, from the work of Wittmaack & Poker (1990) it is known that the decay length for ^{28}Si in ^{30}Si is the same as for ^{30}Si in ^{28}Si. This implies that any unidirectional contribution to collisional relocation such as recoil implantation must be undetectably small. Hence the apparent centroid position of the ^{30}Si-δ in ^{28}Si equals $\langle z\rangle \approx \langle z\rangle_{\mathrm{is}} + z_{\mathrm{or}}$, and z_{d}^0 can be determined using (3.6). The 'only' requirement is a safe evaluation z_0 by way of extrapolation to the limit $E = 0$. The close agreement in the energy dependence of the apparent centroid positions for B and Si-δ tracers then implies that boron deltas can be used as a secondary standard for determining z_{d}^0.

In terms of profile shift and broadening, boron in oxygen bombarded silicon constitutes a very favourable case (negligible unidirectional shift, small decay length). Other common silicon dopants are much less well-behaved. Apparent centroid positions for B-, Ge- and Sb-spikes in Si are compared in figure 9*b* (Dowsett *et al.* 1992). Unfortunately, the scatter in the data for Ge and Sb does not allow a safe extrapolation to vanishing beam energy. Nevertheless the differential shift $\mathrm{d}\langle z\rangle/\mathrm{d}E$ for the

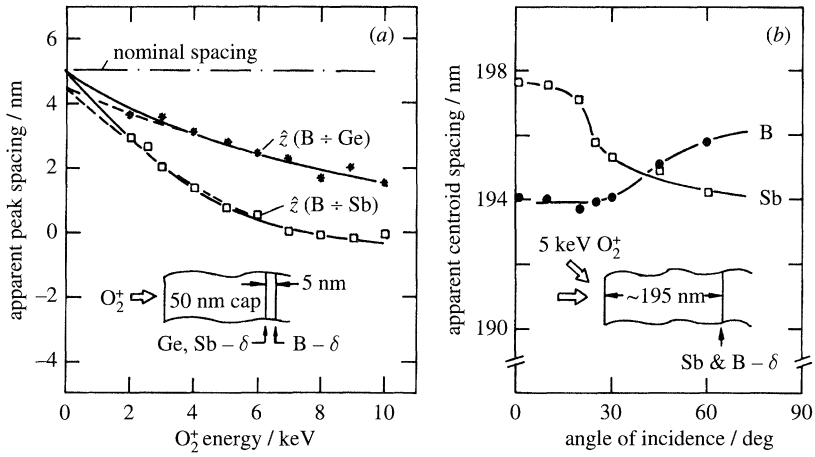

Figure 10. (*a*) Impact-energy dependence of apparent peak spacings between Ge-, Sb- and B-δs, profiled at normal O_2^+ incidence. The sample structure is sketched in the insert (Dowsett *et al.* 1994). (*b*) Apparent centroid spacing of codeposited B- and Sb-δs versus the angle of O_2^+ incidence (Wittmaack 1994*b*).

Ge-δ is clearly (about 30%) less than for the B-δ. This implies some unidirectional transport of Ge away from the surface. The effect is very pronounced for the Sb-δ in which case the apparent profile shift due to the depth scale offset is (almost) completely balanced by the chemically driven impurity transport. Without a detailed knowledge of the different sources of apparent and real impurity relocation, depth profiling of Sb-δ spikes at different beam energy could erroneously suggest that there is no profile shift but 'merely' a bombardment induced profile broadening.

The magnitude of chemically driven impurity transport has been explored in more detail on samples containing one or more deltas of boron and of some other impurity, the former serving as a reference species. Using this approach the accuracy in determining the relative shift can be improved considerably. Figure 10*a* shows the impact energy dependence of the apparent peak separation for combinations of B/Ge and B/Sb, with a nominal spacing of 5 nm (Dowsett *et al.* 1994). The results substantiate the conclusions derived from figure 9*b* (if apparent centroid spacings had been plotted in figure 10*a* the effect would be larger because the decay length for Ge and Sb are significantly larger than for B).

Note that extrapolation of the experimental data to $E = 0$ (dashed lines in figure 10*a*) yields a 'true' delta spacing of 4.5 nm, i.e. 10% less than the nominal spacing. This deviation could be due to a corresponding uncertainty in thickness determination from MBE growth parameters. Alternatively one could argue that the escape probability of B atoms is higher than of Ge and Sb atoms. According to figure 3*b* this would make the apparent peak spacing smaller because the latter species were located before the former (see insert of figure 10*a*). Conclusive evidence in this respect may be obtained from experiments on samples containing the tracers in different order (but with the same spacer thickness).

The pronounced relocation of Ge and Sb atoms is intimately related to the fact that a constantly renewed oxide layer is present at the surface of silicon when bombarded with oxygen at near-normal incidence. If depth profiling is performed at angles larger than 25–35° (depending on energy), a continuous oxide cannot be formed any more and the chemical effect disappears gradually. This angular dependence is illustrated

PHILOSOPHICAL TRANSACTIONS OF THE ROYAL SOCIETY A MATHEMATICAL, PHYSICAL & ENGINEERING SCIENCES

in figure 10*b*, which shows apparent centroid spacings for codeposited B and Sb-δs. The original data (Wittmaack 1994*b*) have been corrected for a 6 nm depth scale offset (for less than 30°), which, however, reduces to 1.5 nm owing to the special depth calibration procedure applied in that study. In general accordance with figure 10*a* the Sb/B centroid spacing is large at normal incidence, but is almost undetectable at angles between 35 and 50°. At more oblique incidence the B-δ is apparently shifted deeper into the silicon host matrix. This could be due to recoil implantation, a process that may become observable only at relatively large angles (and relative to Sb), the reason being as follows. The close similarity in the masses of projectile (^{16}O) and impurity atoms (^{11}B) provides efficient transfer of energy and momentum (compared to Sb). The associated boron relocation is, however, masked at angles less than about 30° because the oxygen subsystem in the beam synthesised SiO_2 acts as a buffer for collisional relocation (Wittmaack & Wach 1981; Wittmaack 1994*a*).

For the sake of completeness we mention that interaction of dopants during sputter profiling has been considered a possible process (Dowsett *et al.* 1994). Available data do not appear to be conclusive in this respect. If this kind of interaction were to play a role, one should not only see an effect on the spacing of the centroids but also a change in the decay length (especially if the peak of one tracer profile were located in the tail region of the other).

6. Brief note on the importance of sample quality

It is important to realize that measurements of beam induced broadening and of profile shifts can be significantly in error if the sample is not of very high quality. Probably the most important parameter is the initial surface roughness (to be distinguished from the statistical roughness that may be produced by ion bombardment). Polished silicon wafers of industrial quality are usually very smooth with a mean roughness on the atomic scale. Low-energy implantation distributions in such samples are well suited for measuring decay length (Wach & Wittmaack 1982*b*). However, in order to determine the complete effect of beam induced broadening in the form of a resolution (response) function (Clegg & Gale 1991; Wittmaack 1992; Dowsett *et al.* 1994), one needs buried delta doping tracers. The most simple way of producing such samples is to deposit a very thin layer of the tracer material on a polished substrate and to bury this tracer under a sufficiently thick cover of substrate material. There are two major problems with this approach: At the elevated temperatures required for MBE one may encounter tracer segregation into the growing cap (Zalm *et al.* 1991). Moreover, random and step effects in delta layer growth may lead to a broadened distribution of the tracer atoms about a mean plane. At low (room) temperature vapour deposition may result in island growth and a correspondingly rough surface of the epilayer. In the extreme case of a cap containing pin holes the apparent decay length may be 15 times larger than the value observed with a high-quality sample (Dowsett *et al.* 1994).

Probably the best method of assessing the amount of roughness on a sample produced by growing different layers on an initially flat surface is to determine the front-end steepness of the respective delta profile. According to computer simulations of profile broadening (King & Tsong 1984; Badheka *et al.* 1990) the leading edges are very sharp, provided they are determined by collisional mixing alone. One can choose the input parameters of simulated profiles so as to produce the same decay length as in the measured profiles. If in such a case the leading edge of the

PHILOSOPHICAL TRANSACTIONS OF THE ROYAL SOCIETY A MATHEMATICAL, PHYSICAL & ENGINEERING SCIENCES

experimentally observed profile is broader than the one simulated under the assumption of a smooth surface, it is fairly safe to attribute the enhanced broadening to an intial roughness of the analysed sample (Badeheka *et al.* 1990; Wittmaack 1994*a*).

In future experiments it would be desirable to characterize the surface roughness by independent means, for example by atomic force microscopy. Without this additional piece of information one can only assess the sample quality in terms of roughness by comparing the width of the leading edge of delta profiles (Wittmaack & Poker 1990). Instead of the width the upslope lengths λ_u is often used as a broadening parameter. Characterization of profiles in terms of λ_u is based on the observation that, much like the long range tail, a sizable part of the leading edge can also be described approximately by an exponential depth dependence, $I \propto \exp(z/\lambda_u)$. The steep rise in the δ-profile of figure 4 for 1.5 keV O_2^+ corresponds to $\lambda_u = 0.3$ nm. This very small upslope length implies that the surface of the sample was very smooth. Other samples used in previous work were apparently rather rough. For 2 keV, i.e. almost the same beam energy as in figure 4, the observed upslope lengths ranged from 0.65 nm (Wittmaack 1994*b*) through 0.9 nm (Dowsett *et al.* 1992) to as large as 2.2 nm (Clegg 1987). It is only from the analysis of such samples as in figure 4 that we know how steep the leading edge of delta profiles can be if the surface is (presumably) smooth on an atomic scale.

7. Angular dependence of profile shifts and transition depths

With reference to figure 7 it has been mentioned that the transition depth increases as the bombardment angle θ is changed from near-normal to 45°. A detailed study on the dependence $z_{tr}(\theta)$ has been carried out by Vandervorst & Shepherd (1985, 1987) and Vandervorst *et al.* (1985). Profile shifts were measured using As implantation distributions in Si. An example for an implantation energy of 50 keV and SIMS analysis by 10 keV O_2^+ at 30° is depicted in figure 11*a* (Vandervorst *et al.* 1985). The transition depth was evaluated by determining the time at which the Si^+ signal has reached the stationary level (vertical dashed line in figure 11*a*). Considering the fact that the most probable range for the 50 keV As distribution is (38 ± 2) nm, we conclude that z_{tr} must have been quite large, between 24 and 28 nm. However, in the compilation of $z_{tr}(\theta)$ (see figure 11*b*), the data point relating to this experiment shows up at only 20 nm. Moreover, the transition depth for normal incidence at 10 keV is only 10 nm, which is a factor of two less than the number derived from profiles of B-δ spikes and implantation distributions (Wittmaack 1996*a*). This discrepancy is hard to understand unless an error has occurred in the data analysis. We have speculated that Vandervorst *et al.* (1985) have misinterpreted the apparent transition depth as the true transition depth (Wittmaack 1996*a*), but in order to achieve a better understanding of this kind of problem we take another look at the published profiles.

Unfortunately, Vandervorst & Shepherd (1985, 1987) and Vandervorst *et al.* (1985) have presented only the raw profiles, i.e. intensities versus time, although, according to the publications, the crater depth has been determined for each (?) profile measurement. Analysis of the measured profiles in terms of transition depths was carried out by determining the depth difference between the transition point and the peak position, in which region the erosion rate should be constant and equal to the number derived from crater depth measurements. This procedure is formally correct, but cannot be very accurate because identification of the exact peak position is subject to large uncertainties. Moreover, if depth calibration is at hand, profiles plotted as a

PHILOSOPHICAL TRANSACTIONS OF THE ROYAL SOCIETY A MATHEMATICAL, PHYSICAL & ENGINEERING SCIENCES

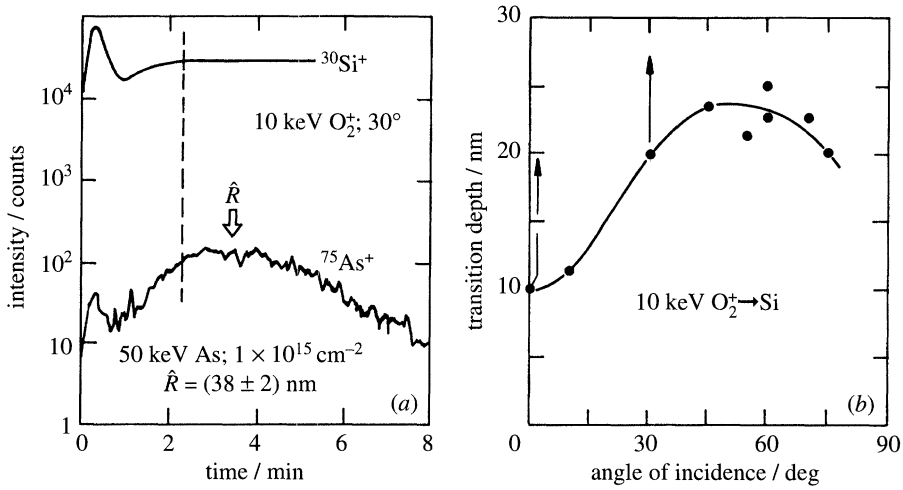

Figure 11. (*a*) Raw SIMS depth profile of As in Si, measured at oblique O_2^+ incidence. The Si^+ matrix signal served to determine the transition time, represented by the vertical dashed line. (*b*) Angular dependence of the transition depths at 10 keV (Vandervorst *et al.* 1985).

function of the apparent depth would immediately provide information about a likely profile shift, as shown in the early work of Wittmaack & Wach (1981). Surprisingly, such numbers have not been quoted for profiles like the one in figure 11*a*.

In order to see whether the results for the As distributions are in accordance with the large amount of data for boron tracers, we make use of As profiles obtained by the same group at low and high probe energies. Figure 12*a* shows a 40 keV As profile measured with 8 keV O_2^+ at 2° (Vandervorst & Shepherd 1987). The same As implantation distribution has also been analysed at a low probe energy of 1.85 keV (dashed curve in figure 12*b*), i.e. the same conditions as those employed to measure the profile in figure 7*b* (Vandervorst *et al.* 1984). The full curve in figure 12*b* is the same as in figure 12*a*. The erosion rate was obtained by fitting the large-depth half width of the full curve to the dashed curve. In essence this is the same procedure as the one that the authors claimed to have used. In addition to this indirect depth calibration the peaks of the two profiles have been made to coincide. Finally a shift of 2.7 nm (labelled z') has been added to the dashed curve (see discussion of figure 7*b*). With this procedure the transition depth for 8 keV O_2^+ at 2°, determined from the position of the local minimum of the As profile, is found to be (17 ± 2) nm, in very good agreement with results obtained from boron tracers (Wittmaack 1996*a*).

We conclude that the numbers shown in figure 11b are not correct in quantitative terms. However, from the work of Clegg (1987) and the analysis presented here there can be little doubt that the transition depth increases with increasing impact angle, at least up to 45°. Accurate measurements of the angular dependence are desirable in order to get a reasonable understanding of the changes in oxygen build-up that seem to occur when going from full to partial oxidation by changing the impact angle.

8. Modelling of bombardment induced oxidation and surface movement

The problem of modelling transient phenomena in oxygen bombarded silicon may be split into two parts. First, one would like to calculate the fluence dependent

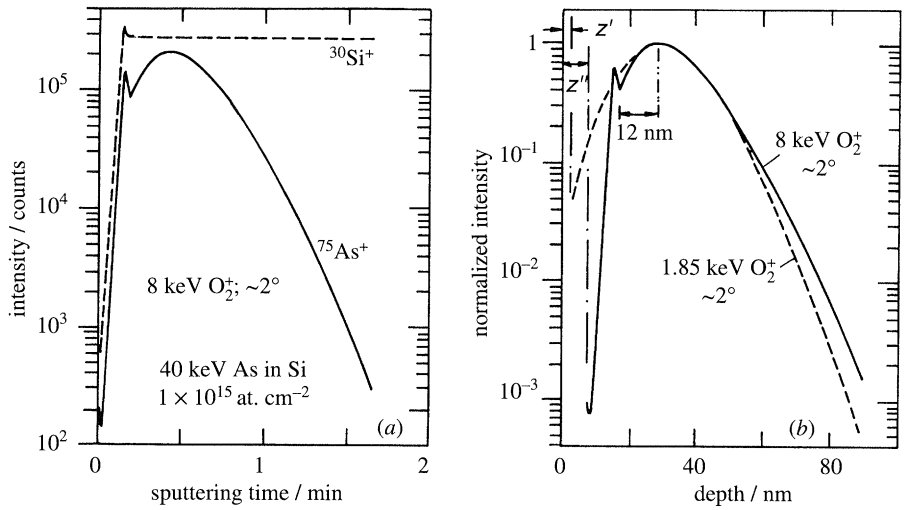

Figure 12. (*a*) Raw SIMS depth profile of As in Si measured at near-normal 8 keV O_2^+ incidence (Vandervorst & Shepherd 1987). (*b*) The same profile after sputter rate evaluation based on a calibrated profile measured by bombardment with 1.85 keV O_2^+ (Vandervorst *et al.* 1984). For details of the evaluation procedure see text.

changes in the partial sputtering yield of silicon and the concurrent changes in the volume of the oxygen loaded regions of the sample ('swelling'). Second, it would be desirable to derive a quantitative description of the oxygen induced increase in ionization probability of sputtered atoms and molecules. The latter issue appears to be the more difficult one because it is necessary to know the oxidation states of matrix and impurity atoms in the outermost layer of the receding surface. Investigations into these problems have been performed using X-ray photoelectron spectroscopy (XPS), but for silicon matrix atoms only (Yu 1991; Alay & Vandervorst 1992). One can also argue that the escape depth of photoelectrons is too large to provide the required information about the composition of the first two layers at the surface. This may hold true even for angular dependent XPS measurements if instruments with large acceptance cones are being used (Alay & Vandervorst 1992). In view of these limitations we will discuss only the transient changes in sputtering yield and surface position.

To model the depth scale offset and the surface movement produced by oxygen bombardment it is necessary to have a quantitative knowledge of several input parameters. During the transient period two of these parameters will undoubtedly go through a fluence dependent change, the (partial) sputtering yield of silicon, $Y = Y(\Phi)$, (Si atoms per O atom), and the differential oxygen retention (accommodation) coefficient $\alpha = \alpha(\Phi)$. More difficult to answer is the question whether the volume occupied by silicon atoms, Ω_{Si} (cm^3 atom^{-1}), is affected by the presence of oxygen atoms. Similarly we do not know whether the atomic volume of oxygen, Ω_{O_x}, is a function of the oxygen concentration or the binding state, or whether an isolated oxygen atom in Si and oxygen in SiO_2 occupy the same volume. Only the end point of the oxidation process is known in terms of the volume occupied by SiO_2 molecules, Ω_{SiO_2} (cm^3 molecule^{-1}). Since relevant information is not available, we have to make the assumption that Ω_{Si} and Ω_{O_x} are independent of the oxygen concentration. This is equivalent to the idea that all the implanted oxygen immediately reacts with silicon to form SiO_2, an assumption often made in modelling beam induced oxidation

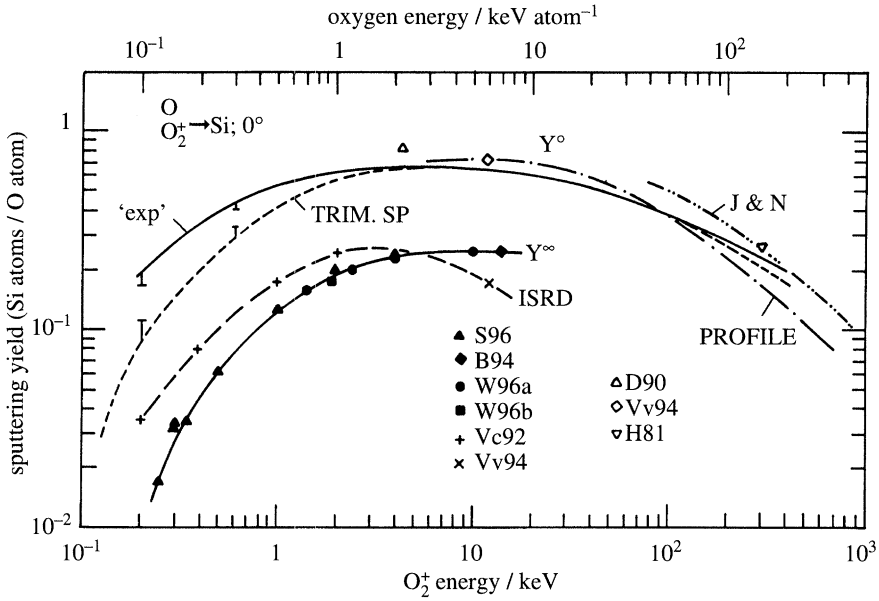

Figure 13. Initial and stationary sputtering yield of oxygen bombarded silicon, compiled from various sources (see text): S96 (Smith *et al.* 1996); B94 (Beyer 1994); W96*a*, *b* (Wittmaack 1996*a*, *b*); Vc92 (Vancauwenberghe 1992); Vv94 (Vandervorst *et al.* 1994); D90 (Dowsett *et al.* 1994); H81 (Hayashi *et al.* 1981).

(Todorov & Fossum 1988). In either case it suffices to know Ω_{Si} and $\Omega_{\mathrm{SiO_2}}$, and to consider Ω_{O_x} a short-form term for a difference in volume:

$$\Omega_{\mathrm{O}_x} \equiv \tfrac{1}{2}(\Omega_{\mathrm{SiO_2}} - \Omega_{\mathrm{Si}}). \tag{8.1}$$

The right-hand side may interpreted as the difference between the volume produced and the volume consumed, per incorporated oxygen atom that forms an SiO_2 bond. For crystalline silicon, $\Omega_{\mathrm{Si}} = 2.0\times10^{-23}$ cm^3, and for vitreous silicon dioxide, $\Omega_{\mathrm{SiO_2}} = 4.4 \times 10^{-23}$ cm^3. Differences in atomic volume between amorphous and crystalline silicon can be ignored because the former has been found to be only 1.8% less dense than the latter (Custer *et al.* 1994).

As to the the initial sputtering yield Y^0, only two experimental data have been reported at low energies (Dowsett *et al.* 1990; Vandervorst *et al.* 1994) and another one for a relatively high energy of 150 keV atom^{-1} (Hayashi *et al.* 1981). One can derive reasonably accurate numbers by interpolation of data for inert gas ion bombardment (Wittmaack 1996*a*) as shown in figure 13 (full line labelled 'exp'). Similarly one can interpolate results of TRIM.SP computer simulations (Eckstein 1989, Eckstein *et al.* 1993). Sputtering yield simulations relating directly to oxygen bombardment have been performed using the PROFILE code (Li *et al.* 1991) and another unspecified code, labelled J&N (Jäger 1986).

The stationary sputtering yield is easy to measure and results have been reported by many groups. Some of the more recent data are presented in figure 13 (Beyer 1994; Smith *et al.* 1996; Wittmaack 1996*a*, *b*). Also shown are theoretical results obtained by the ion beam oxidation–sputtering simulation program ISRD in combination with a modified TRIM code (Vancauwenberghe 1992; Vancauwenberghe *et al.* 1992; Vandervorst *et al.* 1994), an approach that will be discussed in more detail later. Considering only the experimental data we see that the ratio Y^0/Y^∞ increases

from about 10 at the lowest energies to 2.5 for 10 keV O_2^+. The concurrent variation in the yield difference $Y^0 - Y^\infty$ ranges from 0.1 to 0.4 Si atoms per O atom.

To the author's knowledge experimental data on the accommodation coefficient for oxygen in silicon are not available. Theoretical data for $\alpha^0 = \alpha(\Phi \to 0)$ may be derived by interpolation of results from TRIM.SP simulations (Eckstein & Biersack 1986). At about 100 keV atom^{-1} essentially all implanted species are retained ($\alpha^0 > 0.99$). As the energy is reduced, α^0 decreases slowly and amounts to about 0.93 at 1 keV atom^{-1}.

In order to model bombardment induced changes in sputtering yield and oxygen retention, for example with TRIM.SP, it would be necessary to have an accurate knowledge of the diffusion and oxidation kinetics under ion bombardment. At present the required knowledge is not available in sufficient detail. Given this situation it is tempting to explore the quantitative aspects of the oxidation–sputtering process by combining the assumptions outlined above with simple analytical expressions for $Y = Y(\Phi)$ and $\alpha = \alpha(\Phi)$. Such an analytical sputtering–oxidation model (ASOM) has been explored recently (Wittmaack 1996*a*). The results are described here in a more general form. First we recall that the depth scale offset z_d^0 is generated because initially the sputtering yield exceeds the stationary value by the amount $\Delta Y(\Phi) = Y(\Phi) - Y^\infty$. Hence the *excess* thickness Δz_{Si} sputtered during the transient period is, for $\Omega_{Si} = \text{const.}$,

$$\Delta z_{Si}(\varphi) = \Omega_{Si}\,\Phi_{tr} \int_0^\varphi \Delta Y(\varphi')\,\mathrm{d}\varphi', \tag{8.2}$$

where, for convenience, we have written the fluence in reduced units, $\varphi = \Phi/\Phi_{tr}$. The offset is the total excess thickness

$$z_d^0 = \Delta z_{Si}(\varphi = 1). \tag{8.2\,a}$$

Counting surface recession positive, the contribution of retained oxygen to the thickness of the implanted sample is

$$z_{O_x}(\varphi) = -\Omega_{O_x}\,\Phi_{tr} \int_0^\varphi \alpha(\varphi')\,\mathrm{d}\varphi' \tag{8.3}$$

and

$$w_{O_x} \equiv -z_{O_x}(\varphi = 1) = \eta\Omega_{O_x}\,\Phi_{tr}. \tag{8.3\,a}$$

The fractional and the mean oxygen retention coefficients, η_f and η, respectively, are defined as

$$\eta_f(\varphi) = \int_0^\varphi \alpha(\varphi')\,\mathrm{d}\varphi' \tag{8.4}$$

and

$$\eta \equiv \eta_f(\varphi = 1). \tag{8.4\,a}$$

The coefficient η can be determined from the stationary areal density of oxygen,

$$D_{O_x}^\infty = \eta\,\Phi_{tr}, \tag{8.5}$$

or the equivalent in terms of oxide thickness

$$w_{SiO_2} = 0.5\eta\Omega_{SiO_2}\,\Phi_{tr} = 0.5\Omega_{SiO_2} D_{O_x}^\infty. \tag{8.5\,a}$$

At this point ASOM invokes the additional assumption that the relative change in

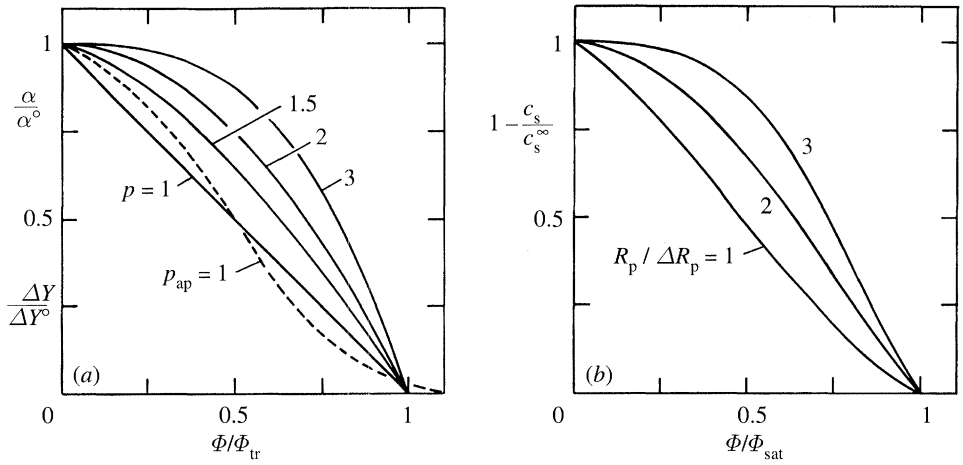

Figure 14. Theoretical fluence dependence of (*a*) the scaled accommodation coefficient and the relative excess sputtering yield and (*b*) the normalized silicon surface concentration. The parameters in (*a*) and (*b*) are the power p of (8.6) and the relative oxygen range, respectively.

sputtering yield is the same as the relative change in the differential oxygen retention coefficient α, and that these changes can be described by a simple analytical expression of the form

$$\alpha(\varphi)/\alpha^0 = \Delta Y(\varphi)/\Delta Y^\infty = 1 - \varphi^p, \quad \text{for } \varphi \leqslant 1, \tag{8.6}$$

where $\Delta Y^\infty = Y^0 - Y^\infty$. For $\varphi \geqslant 1$ the oxygen content of the sample remains constant and there is no excess sputtering any more, i.e. $\alpha(\varphi \geqslant 1)/\alpha^0 = \Delta Y(\varphi \geqslant 1)/\Delta Y^\infty = 0$. The free parameter in (8.6) is the exponent p which is a measure of the 'speed' at which α and Y change at the onset of bombardment. At low energies the implantation distributions are broad ($\Delta R_p/R_p$ relatively large) and p can be assumed to be close to unity (see figure 14*a*). As the oxygen energy increases, $\Delta R_p/R_p$ decreases and the oxygen concentration at the surface will initally increase only slowly. This feature can be described by $p > 1$.

One might argue that describing the process of oxygen implantation by a single parameter is too simple an approach. In order to check the relevance of the approach we consider the predictions of a frequently cited model of ion collection in the presence of sputtering (Schulz & Wittmaack 1976). The key parameters therein are α^0, Y and $R_p/\Delta R_p$. The model allows the surface concentration ratio, c_s, of implanted versus host atoms to increase to an upper limit which depends only on the sputtering yield, $c_s^\infty = \alpha^0/Y$ (or $c_s^\infty Y = \alpha^0$). Solubility limits were not taken into account. With $\alpha^0 \approx 1$ and $Y = Y^\infty \leqslant 0.25$ Si atoms per O atom (see figure 13), this would lead to an unreasonably high limit $c_s^\infty \geqslant 4$, as opposed to the thermodynamically stable ratio $c_s^\infty = 2$ (for SiO_2). To account for this, we have imposed an upper limit $c_s^\infty Y = 0.7$ to the build-up curves of the collection model, by which procedure a saturation fluence Φ_{sat} is also defined. For comparison with figure 14*a* the modified theoretical results are presented as plots of the reduced change in silicon surface concentration, $1 - (c_s/c_s^\infty)$, versus the reduced fluence Φ/Φ_{sat} (see figure 14*b*) (c_s/c_s^∞ is the reduced oxygen surface concentration). The similarity of the two sets of curves is evident, thus supporting the idea that (8.6) constitutes a useful basis for modelling the oxygen build-up and the associated sputtering yield changes.

For completeness we mention that the shapes of the curves in figure 14*b* change

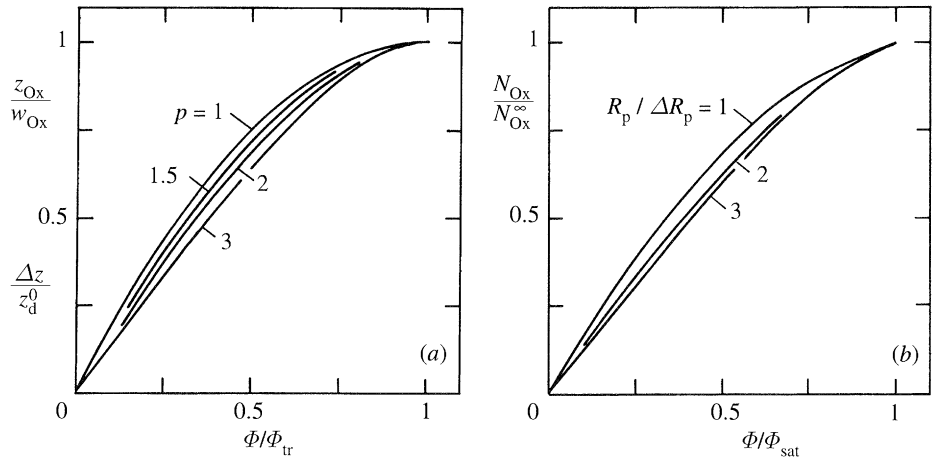

Figure 15. The same as figure 14 but for (*a*) the relative oxygen 'thickness' and the relative depth scale offset and (*b*) the relative oxygen content.

only very little if the 'cut-off' $c_s^{\infty}Y$ is varied between 0.5 and 0.7. These numbers happen to be equal to the mean retention coefficients derived from experimental data for oxygen energies between 0.5 and 20 keV atom^{-1} (Wittmaack 1996*a*). It is in fact quite reasonable to consider $c_s^{\infty}Y$ an adjustable parameter that should be set equal to experimentally determined values of η rather than to the differential retention coefficient which, in the collection/sputtering model, has been assumed to be equal to α^0 throughout the whole transient period, irrespective of c_s.

Using (8.6) we can integrate (8.2) and (8.3) to get

$$\Delta z_{Si}(\varphi)/z_d^0 = -z_{O_x}(\varphi)/w_{O_x} = \{1 + p^{-1}(1 - \varphi^p)\}\varphi \tag{8.7}$$

and, with (8.2*a*),

$$z_d^0 = (\eta/\alpha^0)(Y^0 - Y^{\infty})\Omega_{Si}\,\Phi_{tr}, \tag{8.8}$$

where

$$\eta/\alpha^0 = p/(1 + p). \tag{8.9}$$

The important aspect of (8.9) is that, by combining experimental data for η with theoretical data for α^0, the exponent is no longer an adjustable parameter.

The scaling factor $p/(1 + p)$ in (8.9) has a simple meaning. It is nothing but the area under the curves in figure 14*a* and $(\eta/\alpha^0)(Y^0 - Y^{\infty}) = \{p/(1 + p)\}(Y^0 - Y^{\infty})$ in (8.8) may be considered a mean excess sputtering yield that is operative during the transient period. This implies that the actual shape of the curves is not a critical factor. For example, the sputtering yield variation according to the dashed curve labelled p_{ap} in figure 14*a* will produce the same offset as the variation represented by the straight line. It is also evident from the dashed curve that Φ_{tr} must not be an accurately defined fluence. A gradual rather than a sharp transition, $\Delta Y(\Phi) \to 0$ and $\alpha(\Phi) \to 0$, will not change the essential features of ASOM. The only number that counts for the depth scale offset is the integral effect of the excess sputtering yield. Describing the transient phenomena in terms of a well defined threshold Φ_{tr} is only an approximation which is in reasonable accordance with experimental observations.

Build-up curves of the excess thickness and the oxygen content derived from (8.7) are shown in figure 15*a* with p as a parameter. In *reduced form* the curves differ comparatively little. The same holds true for build-up curves of the oxygen content

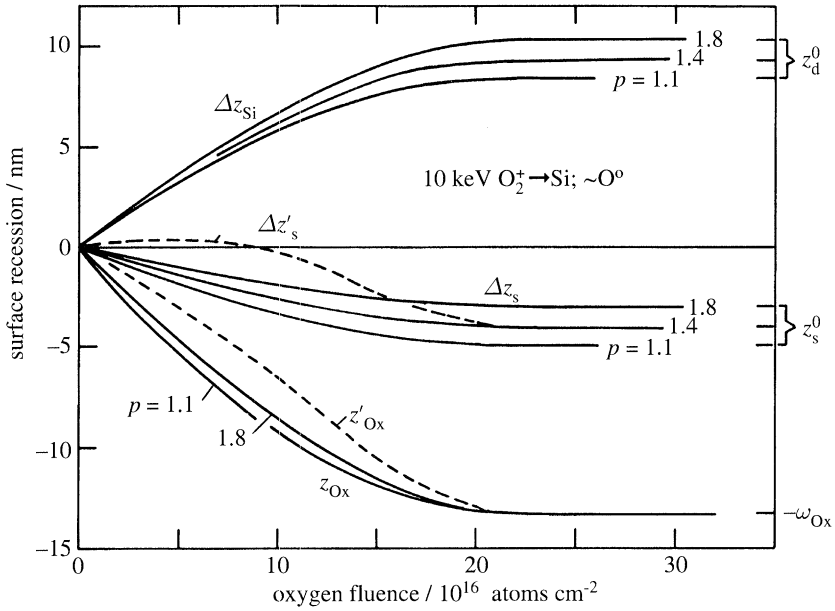

Figure 16. Oxygen-fluence dependence of the excess silicon thickness, the surface position and the oxygen 'thickness' calculated from ASOM for different values of the parameter p. The dashed curves show a hypothetical fluence dependence for more complex oxidation processes.

evaluated from the original data in the collection–sputtering model by applying the cut-off procedure described above (see figure 15*b*).

Turning now from reduced data to absolute numbers, figure 16 shows the fluence dependence of Δz_{Si}, z_{O_x} and the *deviation* Δz_s in the instantaneous surface position, where

$$\Delta z_s(\Phi) = \Delta z_{Si}(\Phi) + z_{O_x}(\Phi) \tag{8.10}$$

and

$$z_s^0 = z_d^0 - w_{O_x}. \tag{8.10\,a}$$

The simulation relates to bombardment of Si with 10 keV O_2^+ at normal incidence. The following input parameters have been used: $Y^0 = 0.65$ Si atoms/O atom, $Y^\infty = 0.25$ Si atoms/O atom, $\alpha^0 = 0.96$, $\eta = 0.56$ (Wittmaack 1996*a*) and $w_{O_x} = \{1 - (\Omega_{Si}/\Omega_{SiO_2})\} w_{SiO_2} = 0.545 \times 24.5$ nm $= 13.4$ nm. The latter number is a rather safe input parameter because the uncertainty in oxide thickness is less than 10%. The quoted values for α^0 and η imply $p = 1.4$. In order to illustrate the effect of varying the exponent in (8.7), results for $p = 1.1$ and 1.8 are also shown. This variation produces a comparatively small 1 nm change of z_d^0 and z_s^0 in either direction ($\pm 11\%$). Hence the quantitative predictions of ASOM do not rest very much on the finer features of the build-up process. The main uncertainty arises from a presently unsatisfactory knowledge of Y^0, but this problem will apply to other models as well.

Note that the surface offset $z_s^0 = (-4.1 \pm 1)$ nm is relatively small compared to the depth scale offset $z_d^0 = (9.3 \pm 1)$ nm. This is the reason why all previous attempts to measure $z_s(\Phi)$ or z_s^0 have apparently failed (Wittmaack 1996*a*). An addional complication may arise from the possibility that the assumption of a constant atomic volume of oxygen may not be fully justified. The net atomic volume may change with the oxidation state of silicon so that the thickness contribution of oxygen will not

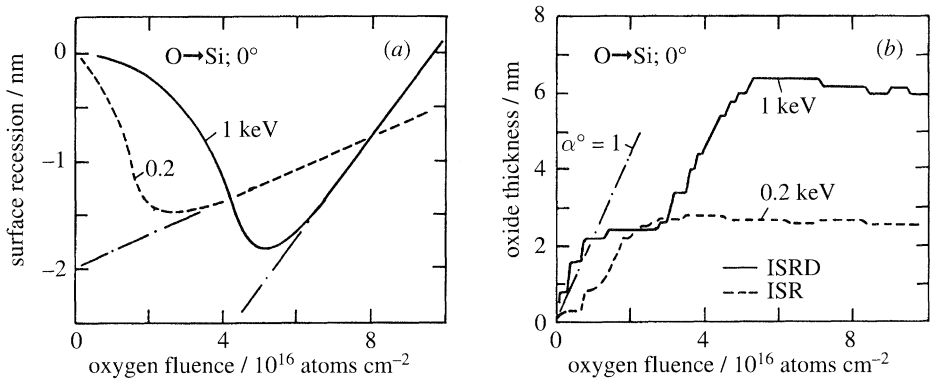

Figure 17. Oxygen-fluence dependence of (*a*) the silicon surface recession and (*b*) the oxide thickness derived from the ISR and ISRD codes (Vancauwenberghe 1992). The codes were identified by the stationary oxide thicknesses given in the cited thesis. The dash-dotted line in (*b*) shows the growth of the oxide thickness expected if all implanted oxygen is converted to SiO_2.

be directly proportional to the retained areal density of oxygen. The net effect of such a complication could be an altered build-up curve of the oxygen 'thickness' as illustrated in figure 16 by the dashed curve labelled z'_{O_x}. This would lead to a situation where initially the excess sputter erosion and the 'swelling' compensate each other almost exactly, i.e. $\Delta z'_s \approx 0$ over a wide range of fluences (hence the true surface position z'_s would initially increase as $\Omega_{Si} Y^\infty \Phi$). Even if in future work the initial surface positions could be measured reliably and with the required accuracy, interpretation of the results could be very difficult.

Beam induced oxidation has also been modelled by an implantation–sputtering–relocation–diffusion computer code ISRD and by reduced versions IS and ISR, all containing TRIM as a subroutine (Vancauwenberghe 1992; Vancauwenberghe *et al.* 1992). Results of this simulation are shown in figure 17 (Vancauwenberghe 1992). Although data presentation and bombardment energies differ somewhat from figure 16, rather significant differences between the predictions of the two models are immediately evident. In IS and ISRD the maximum surface expansion is quite large (almost 2 nm for 1 keV O, see figure 17*a*) and the oxide thickness exhibits an extended plateau around $\frac{1}{3}\Phi_{tr}$ (figure 17*b*, also prominent at 0.5 keV, but not shown here). The latter finding suggests that at some critical oxygen concentration in the sample the code produces an 'outburst' of oxygen, an effect which may be associated with the assumption that excess oxygen in oxidized regions is allowed to migrate freely (and diffuse out). Another problem with the results in figure 17*b* is that the initial oxide growth proceeds faster than expected for $\alpha^0 = 1$ and if the equivalent atomic volume of oxygen, $\Omega_{O_x} = \frac{1}{2}(\Omega_{SiO_2} - \Omega_{Si})$, is set to 1.2×10^{-23} cm^3 (see dash-dotted curve in figure 17*b*). Deviations from this number or concentration dependent changes in atomic and/or molecular volume(s) have not been mentioned in the original publication.

The IS and ISRD predictions also differ from ASOM in terms of z_s^0 and z_d^0. From figure 17*a* we find $z_s^0 = -2$ nm and -4.7 nm, for 0.2 and 1 keV, respectively (the slopes of the straight lines equal the stationary sputtering yields Y^∞ shown in figure 13). By contrast ASOM predicts a surface offset of only -1.4 nm for 1 keV O. Using the IS and ISRD values for z_s^0 and the stationary ISRD thicknesses to calculate z_d^0 according to (8.10 *a*) we find the depth scale offset to be *negative* (!), for example $z_d^0 = -4.7 + 3.2 = -1.5$ (nm) at 1 keV. If this were correct, sputter profiles measured

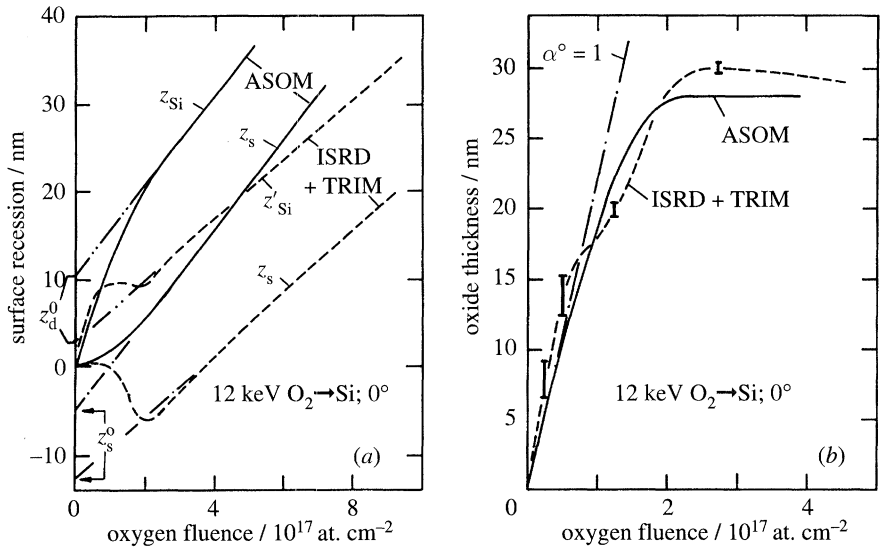

Figure 18. Dashed curves: the same as figure 17, but for a higher implantation energy (Vandervorst *et al.* 1994). The curve denotes the sum of the oxygen 'thickness' and the surface position. The solid curves are results obtained from ASOM.

under bombardment with normally incident oxygen should be shifted *away* from the original surface. The opposite is true, as illustrated by the experimental results of figure 8. In the simulations something appears to have gone wrong with the initial sputtering yield as with the oxygen (out) diffusion.

The ISRD code has also been employed by Vandervorst *et al.* (1994) to simulate oxidation and swelling at a relatively high energy (12 keV O_2^+). The general features of the results (dashed curves in figure 18) are essentially the same as in figure 17. There are only differences in the absolute numbers. Again z_s^0 is very large (−12.5 nm) and consequently, z_d^0 rather small (3 nm), but positive as it should be. However, the latter number is almost a factor of four lower than experimentally observed shifts and also lower by this factor than the number (10.4 nm) derived from ASOM (solid lines in figure 18). Moreover, the surface offset predicted by ISRD is so large that it should easily be detecable by surface profilometry. But most of the published data on crater depth measurements do not support this prediction (Wittmaack 1996*a*).

We are thus forced to conclude, that the ISRD code in its present form produces erroneous results. The only apparent success reported in the past relates to the prediction of oxide thicknesses versus oxygen energy. This was achieved by a trial-and-error optimization of the assumed transport and diffusion parameters until, at one energy, the simulated thickness agreed with the experimental result. The authors (Vancauwenberghe 1992; Vancauwenberghe *et al.* 1992) have not reported on consistancy checks relating to features other than the oxide thickness and they have not explained such observations as the plateau in figure 17*b*. Results of depth profiling experiments were not taken into account. It was claimed that there is good agreement with results of the I-S model of beam induced oxidation (Todorov & Fossum 1988). However, a closer look at the simulated oxide profiles shows that there is complete disagreement in such important details as the width of the interface. In ISRD the simulated interface is very sharp (*ca.* 0.3 nm for 100 eV O), as opposed to the I-S model which predicts a width that is almost 10 times as thick (2.5–3 nm for 100 eV O_2). Whereas the former result is at variance with experimental observations the lat-

ter shows the right trend. A direct comparison of measured and simulated interface width for the same bombardment conditions has not been performed, but analysis of a fully oxidized sample by cross sectional transmission electron microscopy and sputter profiling in combination with Auger electron spectrscopy (Augustus *et al.* 1988) revealed a broad SiO_x ($x < 2$) transition layer between the oxide and the silicon substrate (*ca.* 7 nm thick for 4 keV O_2). Depth profiling measurements suggest that the interface width varies only slowly with the beam energy (Wittmaack 1994*c*). If we assume that the width is proportional to the oxide thickness, the ratio of the widths for 4 versus 0.1 keV O_2 would be 3.4 ± 0.3. This is not too far from the ratio (2.3 . . . 2.8) of the experimental and theoretical interface width quoted previously.

Finally we mention that the difference $\Delta = \{z_{Si}(\Phi) - z_s(\Phi)\}_{\Phi > \Phi_{tr}}$ has been claimed to equal the profile shift (Vandervorst *et al.* 1994). This is not correct. The apparent profile shift is a number that is related to the initial excess silicon sputter removal and the inablity to measure the associated depth calibration error by surface profilometry. As one can tell from figure 18*a*, the shift or, more correctly, the depth offset z_d^0 is found by extrapolating the linear section of $z_{Si}(\Phi)$ to zero fluence. Alternatively z_d^0 can be determined from Δz_{Si} ($\Phi > \Phi_{tr}$), as has been illustrated in figure 16. The depth difference Δ is nothing but the excess thickness w_{O_x} due to oxygen incorporation, i.e. $\Delta \equiv w_{O_x}$. The authors may have been led to the incorrect interpretation of Δ because the differential change in oxygen 'thickness', dw_{O_x}/dE ($= 1.14\,\text{nm keV}^{-1}\,\text{atom}^{-1}$), happens to be close to the experimentally observed differential profile shift dz_{sh}/dE (*ca.* 0.9 nm keV^{-1} atom^{-1}) (see figures 8 and 9).

9. Compilation of characteristic transition parameters

Experimental data for the apparent transition depth z_c, the profile shift z_{sh} and the total (or true) transition depth $z_{tr} = z_c + z_{sh}$ are compiled in figure 19. The data relate to oxygen bombardment at normal or near-normal beam incidence ($\theta \leqslant 5°$). Also shown is the depth scale offset z_d^0 calculated from (8.8). In view of the uncertainties concerning the magnitude of the initial sputtering yields Y^0 at energies below 1 keV atom^{-1} (see figure 13), the offset has been evaluated for the upper and the lower limits, labelled 'exp' and TRIM, respectively. Combining experimental data for the oxide thicknesses w_{SiO_2} (or the fraction w_{O_x}) with calculated data for z_d^0 we may also derive numbers for the surface offset z_s^0 (see (8.10 *a*)). Finally, the z_d^0 values have also been combined with experimental z_c data to derive 'calculated' values for the total shift $z_c + z_{sh}$ and the total transition depth $z_c + z_d^0$.

It is evident from the full symbols in figure 19*a* that there is rather good agreement between the shift values measured by different groups. To first order we can draw a straight line through the data points, which suggests a power law dependence, $z_h = aE_{O_2}^k$, with $a = 1.2$ nm, E_{O_2} in keV and $k = 0.88$, but in view of the experimental uncertainties a simple linear dependence with $a = 1$ nm would also fit the data. For O_2^+ energies between 5 and 15 keV the calculated offset values and the measured shifts agree quite well. At lower energies the calculated data are too high, but if TRIM values for Y^0 were correct, the discrepancy is almost within the experimental uncertainties. One should also note that z_d^0 is directly proportional to the mean oxygen retention coefficient η, see (8.8), and that measured η values are not very accurate at low energies.

Considering the simplicity of the assumptions that have been used in the ASOM approach, the agreement between z_d^0 and z_{sh} is surprisingly good. It must be pointed

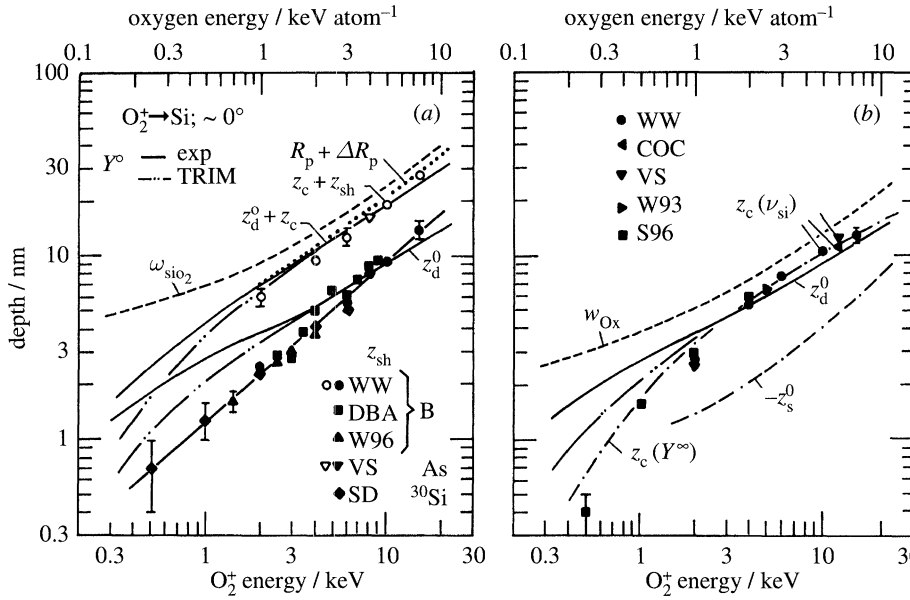

Figure 19. Compilation of the energy dependence of transition, range and thickness parameters for oxygen bombardment of silicon at near-normal incidence. The solid and dash-(double) dotted curves were derived from ASOM. The open and full symbols represent experimental data: WW (Wittmaack & Wach 1981); DBA (Dowsett *et al.* 1994); W96 (Wittmaack 1996*a*); VS, evaluated from Vandervorst & Shepherd (1987); SD (Smith *et al.* 1996); COC (Clegg & O'Connor 1981); W93 (Wittmaack 1993); S96 (Smith 1996).

out, however, that in its present form ASOM is mainly meant to connect experimental data from different sources. In fact, (8.8) should be viewed as an equation that relates the apparent shift observed in sputter depth profiling experiments to other experimentally observable quantities, the initial and final sputtering yields, the oxide thickness and the transition fluence. In other words, ASOM constitutes an attempt to derive an internally consistant picture of beam induced oxidation and the transient phenomena in SIMS.

According to (8.5 *a*) and (8.8) we have $z_d^0 \propto (Y^0 - Y^\infty)\eta\Phi_{tr} \propto (Y^0 - Y^\infty)w_{SiO_2}$. As $(Y^0 - Y^\infty)$ is roughly constant over a wide range of O_2^+ energies, from about 2 to 15 keV, z_d^0 exhibits almost the same energy dependence as w_{SiO_2} or w_{O_x} (see figure 19). At energies below 2 keV, however, $(Y^0 - Y^\infty)$ as well as Y^∞ decrease rapidly with decreasing energy (figure 13). With the aim of minimizing artefacts in SIMS depth profiling this has the important consequence that z_{sh} and z_c also decrease very rapidly towards low energies (the lower the sputtering yield or yield difference, the smaller the thickness that is being sputtered by a given primary ion fluence). As the O_2^+ energy is reduced below (0.75 ± 0.05) keV, both z_{sh} and z_c drop below 1 nm. This number is comparable to or less than the thickness of a typical native oxide on Si. Using probe energies of less than 0.7 keV for depth profiling of *real* (surface oxidized) samples one would thus expect only very small, if not negligible transient effects. In agreement with this supposition the build-up curves in figure 2*b* show very small ion yield changes at 0.5 and 0.25 keV. Transient phenomena can be expected to be observable only on 'artificial' samples, prepared either by etching off the native oxide immediately before sample transfer into the analysis chamber or by in situ sputter cleaning.

Last but not least, figure 19*b* shows the energy dependence of the surface offset $z_s^0 = z_d^0 - w_{O_x}$. In the energy range of interest for SIMS depth profiling (O_2^+ energy less than 5 keV) the offset derived from ASOM amounts to only about −2 nm or less. As pointed out before, this small effect will be very hard to measure with standard surface profilometry equipment. Improved accuracy can be expected by use of atomic force microscopy.

10. Summary and conclusion

This review constitutes an attempt to join together available knowledge on transient phenomena, bombardment induced relocation and beam induced oxidation. These aspects can hardly be understood if they are considered separately. For example, if one wants to determine the true location of a delta doping distribution by SIMS in combination with oxygen bombardment one needs to know both the possible depth scale offset and the beam induced impurity relocation. The problem is that both vary with primary ion energy and impact angle and that the magnitude of relocation is different for different impurities.

At the end of a big effort like this one it is appropriate to ask for the progress that has been achieved since the original discovery of the profile shift phenomenon (Wittmaack & Wach 1981). According to figure 19 the results of the early work agree very well with data reported later on. The achievements made since then may be summarized as follows. (1) Through the use of delta doping distributions it has been possible to identify the finer details of profile broadening effects. Model calculations and computer simulations of depth profiling turned out to be useful, notably with respect to the importance of escape probabilities (preferential sputtering) and the effect of a non-negligible depth of origin of sputtered atoms. (2) The availability of isotopically pure tracer layers of Si in Si has led to significant progress in the understanding of profile broadening. (3) Work carried out since the early 1990s has clearly shown the advantageous properties of the Si(B) system in terms of the similarities in behaviour of the host and the dopant species under depth profiling conditions. For most practical applications silicon isotopes can be replaced by boron tracers as a secondary standard. (4) Much of the quantitative understanding of depth scale and surface offsets achieved on the basis of the ASOM approach rests on the fact that, since a couple of years, reliable numbers for the oxide thickness have become available.

Most of the experimental data discussed and analysed in this review relate to normal beam incidence. The main reason for doing so was that data for oblique incidence are scarce and often not very reliable. In principle, ASOM should be applicable not only to normal but also to off-normal beam incidence, but the input parameters still need to be determined.

The transient effects and the errors in depth calibration previously observed in depth profiling of silicon by normally incident oxygen can be removed to an essentially negligible level by using O_2^+ primary ions at energies of 0.5 keV or less. The alternative approach to this method is oxygen bombardment at more conventional energies between 2 and 3 keV, but at oblique beam incidence (70–80°) and in combination with an oxygen jet. Although this technique is often used for depth profiling, the quantitative aspects in terms of transition depth and depth scale offset have not been investigated. It should be noted that in order to achieve the desired secondary ion yield enhancement it is not sufficient to saturate the surface with adsorbed oxy-

PHILOSOPHICAL TRANSACTIONS OF THE ROYAL SOCIETY A MATHEMATICAL, PHYSICAL & ENGINEERING SCIENCES

gen. As shown many years ago (Wittmaack 1977) oxygen must be incorporated in the silicon sample to produce a very high ionization probability. Evidence for oxygen incorporation has been obtained by RBS (Wach & Wittmaack 1981) and by isotope tracer experiments (Elst *et al.* 1994). As a result of oxidation the (partial) sputtering yield of silicon decreases significantly (Morgan *et al.* 1981), much like the change from Y^0 to Y^∞ under oxygen ion bombardment at normal incidence. Since adsorbed oxygen is not incorporated instantaneously but as a result of bombardment enhanced diffusion (Wach & Wittmaack 1981), stationary conditions in terms of sputtering yield and ionization probability will be achieved only after having passed through a transient period, qualitatively the same as at normal incidence, but quantitatively still to be explored.

I thank M. G. Dowsett for some helpful comments on the manuscript.

References

Alay, J. L. & Vandervorst, W. 1992 XPS analysis of ion-beam-induced oxidation of silicon substrates. *Surf. Interface Analysis* **19**, 313–317.

Andersen, C. A. 1969 Progress in analytic methods for the ion microprobe mass analyzer. *Int. J. Mass Spectrom. Ion Phys.* **2**, 61–74.

Andersen, C. A. 1970 Analytic method for the ion microprobe analyzer. Part II. *Int. J. Mass Spectrom. Ion Phys.* **3**, 413–428.

Augustus, P. D., Spiller, G. D. T., Dowsett, M. G., Kightley, P., Thomas, G. R., Webb, R. & Clark, E. A. 1988 Cross-sectional transmission electron microscopy and Auger electron spectroscopy studies of primary beam damage at the bottom of SIMS craters eroded in Si. In *Secondary ion mass spectrometry SIMS VI* (ed. A. Benninghoven *et al.*), pp. 485–488. Chichester: Wiley.

Avau, D., Vandervorst, W. & Maes, H. E. 1988 Transient effects during SIMS depth profiling with oxygen. *Surf. Interface Analysis* **11**, 522–528.

Badheka, R., Wadsworth, M., Armour, D. G., van den Berg, J. A. & Clegg, J. B. 1990 Theoretical and experimental studies of the broadening of dilute delta-doped Si spikes in GaAs during SIMS depth profiling. *Surf. Interface Analysis* **15**, 550–558.

Barlow, R. D., Dowsett, M. G., Fox, H. S., Kubiak, R. A. A. & Newstead, S. M. 1992 SIMS response functions for MBE grown delta layers in silicon. *Nucl. Instrum. Meth.* B **72**, 442–446.

Beyer, G. P. 1994 A study of ion beam induced artefacts during the SIMS depth profiling of semiconductor matrices. PhD Thesis, University of London.

Clegg, J. B. 1987 Depth profiling of shallow arsenic implants in silicon using SIMS. *Surf. Interface Analysis* **10**, 332–337.

Clegg, J. B. & O'Connor, D. J. 1981 Evaluation of secondary ion mass spectrometry profile distortions using Rutherford backscattering. *Appl. Phys. Lett.* **39**, 997–999.

Clegg, J. B. & Gale, I. G. 1991 SIMS profile simulation using delta function distributions. *Surf. Interface Analysis* **17**, 190–196.

Custer, J. S., Thompson, M. O., Jacobson, D. C., Poate, J. M., Roorda, S., Sinke, W. C. & Spaepen, F. 1994 Density of amorphous Si. *Appl. Phys. Lett.* **64**, 437–439.

Dowsett, M. G., Jeynes, C., Clark, E. A., Webb, R. & Newstead, S. M. 1990 The redistribution of arsenic and germanium in the altered layer formed during SIMS analysis of silicon. In *Secondary ion mass spectrometry SIMS VII* (ed. A. Benninghoven *et al.*), pp. 615–618. Chichester: Wiley.

Dowsett, M. G., Barlow, R. D., Fox, H. S., Kubiak, R. A. A. & Collins, R. 1992 Secondary ion mass spectrometry depth profiling of boron, antimony, and germanium deltas in silicon and implications for profile deconvolution. *J. Vac. Sci. Technol.* B **10**, 336–341.

Dowsett, M. G., Barlow, R. D. & Allen, P. N. 1994 Secondary ion mass spectrometry analysis of ultrathin impurity layers in semiconductors and their use in quantification, instrumental assessment, and fundamental measurements. *J. Vac. Sci. Technol.* B **12**, 186–198.

PHILOSOPHICAL TRANSACTIONS OF THE ROYAL SOCIETY A MATHEMATICAL, PHYSICAL & ENGINEERING SCIENCES

Eckstein, W. 1989 Quantitative predictions of sputtering phenomena. *Surf. Interface. Analysis* **14**, 799–808.

Eckstein, W. & Biersack, J. P. 1986 Reflection of heavy ions. *Z. Phys.* B **63**, 471–478.

Eckstein, W., García-Rosales, C., Roth, J. & Ottenberger, W. 1993 Sputtering data. IPP 9/82, Max-Planck-Institut für Plasmaphysik, Garching.

Elst, K., Vandervorst, W., Bender, H. & Alay, J. 1994 Study of the altered layer formation under oxygen bombardment in combination with flooding. In *Secondary ion mass spectrometry SIMS IX* (ed. A. Benninghoven *et al.*), pp. 617–620. Chichester: Wiley.

Hayashi, T., Okamoto, H. & Homma, Y. 1981 Defects in Si on buried SiO_2 layer formed by very high dose oxygen implantation. *IOP Conf. Ser.* **59**, 533–538.

Kalbitzer, S. & Oetzmann, H. 1980 Ranges and range theories. *Rad. Effects* **47**, 57–72.

King, B. V. & Tsong, I. S. T. 1984 A model for atomic mixing and preferential sputtering effects in SIMS depth profiling. *J. Vac. Sci. Technol.* A **2**, 1443–1447.

Li, Y., Kilner, J. A., Robinson, A. K., Hemment, P. L. F. & Marsh C. D. 1991 Analysis of thin-film silicon-on-insulator structure formed by low-energy oxygen ion implantation. *J. Appl. Phys.* **70**, 3605–3612.

Littmark, U. & Hofer W. O. 1980 Recoil mixing in solids by energetic ion beams. *Nucl. Instrum. Meth.* **168**, 329–342.

Littmark,U. & Hofer, W. O. 1984 The theory of recoil mixing in solids. In *Thin film and depth profile analysis* (ed. H. Oechsner), pp. 159–200. Berlin: Springer.

Morgan, A. E., de Grefte, H. A. M., Warmoltz, N., Werner H. W. & Tolle, H. J. 1981 The influence of bombardment conditions upon the sputtering and secondary ion yields of silicon. *Appl. Surf. Sci.* **7**, 372–392.

Naundorf, V., & Abromeit, C. 1989 Limits of depth resolution for sputter sectioning: moments of tracer depth distribution. *Nucl. Instrum. Meth.* B **43**, 513–519.

Schulz, F. & Wittmaack, K. 1976 Model calculation of ion collection in the presence of sputtering: I. Zero order approximation. *Rad. Effects* **29**, 31–40.

Smith, N. S. 1996 Ultra-low energy SIMS depth profiling. Ph.D. thesis, University of Warwick.

Smith, N. S., Dowsett, M. G., McGregor, B. & Phillips, P. 1996 Rapid low energy depth profiling using SIMS. In *Secondary ion mass spectrometry SIMS X* (ed. A. Benninghoven *et al.*). Chichester: Wiley.

Simons, D. S. 1996 The depth measurement of craters produced by secondary ion mass spectrometry—results of a stylus profilometry round-robin study. In *Secondary ion mass spectrometry SIMS X* (ed. A. Benninghoven *et al.*). Chichester: Wiley.

Svensson, B. G., Mohadjeri, B. & Perović, M. 1994 Surface recession and oxidation of silicon during bombardment by low energy ions. *J. Appl. Phys.* **76**, 3831–3834.

Todorov, S. S. & Fossum, E. R. 1988 Oxidation of silicon by a low-energy ion beam: experiment and model. *Appl. Phys. Lett.* **52**, 48–50.

Vancauwenberghe, O. P. J. 1992 On the growth of semiconductor-based epitaxial and oxide films from low energy ion beams. Ph.D. thesis, Massachusetts Institute of Technology.

Vancauwenberghe, O., Herbots, N. & Hellman, O. C. 1992 Role of ion energy in ion beam oxidation of semiconductors: experimental study and model. *J. Vac. Sci. Technol.* A **10**, 713–718.

Vandervorst, W., Alay, J., Brijs, B., De Coster, W. & Elst, K. 1994 Depth profiling with oxygen beams. In *Secondary ion mass spectrometry SIMS IX* (ed. A. Benninghoven *et al.*), pp. 599–608. Chichester: Wiley.

Vandervorst, W., Maes, H. E. & De Keersmaker, R. F. 1984 Secondary ion mass spectrometry: depth profiling of shallow As implants in silicon and silicon dioxide. *J. Appl. Phys.* **56**, 1425–1433.

Vandervorst, W. & Shepherd, F. R. 1985 Transient effects in SIMS analysis for different angles of incidence of an EMBED primary ion beam. *Appl. Surf. Sci.* **21**, 230–242.

Vandervorst, W. & Shepherd, F. R. 1987 Secondary ion mass spectrometry profiling of shallow implanted layers using quadrupole and magnetic sector instruments. *J. Vac. Sci. Technol.* A **5**, 313–320.

PHILOSOPHICAL TRANSACTIONS OF THE ROYAL SOCIETY A MATHEMATICAL, PHYSICAL & ENGINEERING SCIENCES

Vandervorst, W., Shepherd, F. R., Newman, J., Phillips, B. F. & Remmerie, J. 1985 Surface transient behaviour of the $^{30}Si^{+}$ yield with angle of incidence and energy of an primary beam. *J. Vac. Sci. Technol.* A **3**, 1359–1362.

Wach, W. & Wittmaack, K. 1981 Ion implantation and sputtering in the presence of reactive gases: bombardment induced incorporation of oxygen and related phenomena. *J. Appl. Phys.* **52**, 3341–3352.

Wach, W. & Wittmaack, K. 1982*a* Low energy range distributions of ^{10}B and ^{11}B in amorphous and crystalline silicon. *Nucl. Instrum. Meth.* **194**, 113–116.

Wach, W. & Wittmaack, K. 1982*b* Element-specific broadening effects in SIMS depth profiling of light impurities implanted in silicon. *Surf. Interface Analysis* **4**, 230–233.

Wach, W. & Wittmaack, K. 1983 Ranges of low-energy, light ions in amorphous silicon. *Phys. Rev.* B **27**, 3528–3537.

Wilson, R. G., Stevie, F. A. & Magee, C. W. 1989 *Secondary ion mass spectrometry. A practical handbook for depth profiling and bulk analysis.* New York: Wiley.

Winterbon, B. K. 1975 *Ion implantation range and energy deposition distributions. Low incident energies*, vol. 2. New York: Plenum.

Wittmaack, K. 1977 The use of secondary ion mass spectrometry for studies of oxygen adsorption and oxidation. *Surf. Sci.* **68**, 118–129.

Wittmaack, K. 1981 Oxygen-concentration dependence of secondary ion yield enhancement. *Surf. Sci.* **112**, 168–180.

Wittmaack, K. 1985 Influence of the impact angle on the depth resolution and the sensitivity in SIMS depth profiling using a cesium ion beam. *J. Vac. Sci. Technol.* A **3**, 1350–1354.

Wittmaack, K. 1987 Periodicity of impurity segregation effects in oxygen bombarded silicon. *Nucl. Instrum. Meth.* B **19/20**, 484–487.

Wittmaack, K. 1991 Surface and depth analysis based on sputterung. In *Sputtering by particle bombardment III* (ed. R. Behrisch & K. Wittmaack), pp. 161–256. Berlin: Springer.

Wittmaack, K. 1992 Basic aspects of sputter profiling. In *Practical surface analysis* (Ion and neutral spectroscopy) (ed. D. Briggs & M. P. Seah), 2nd. edn, vol. 2, pp. 105–175. Chichester: Wiley.

Wittmaack, K. 1993 Comparison of the resolution functions for depth profiling of boron and antimony in silicon using oxygen bombardment at different energies and implact angles. In *Proc. 2nd Int. Workshop Measurement and characterization of ultra-shallow doping profiles in semiconductors* (ed. R. Subrahmanyan, C. Osburn & P. Rai-Chouhury), pp. 189–195. Research Triangle Park: MCNC.

Wittmaack, K. 1994*a* Towards the ultimate limits of depth resolution in sputter profiling: beam-induced chemical changes and the importance of sample quality. *Surf. Interface Analysis* **21**, 323–335.

Wittmaack, K. 1994*b* Secondary ion mass spectrometry depth profiling of boron and antimony deltas in silicon: Comparison of the resolution functions using oxygen bombardment at different energies and impact angles. *J. Vac. Sci. Technol.* B **12**, 258–262.

Wittmaack, K. 1994*c* Thickness of SiO2 layers produced by oxygen implantation in Si: a CsAMS depth profiling study. In *Secondary ion mass spectrometry SIMS IX* (ed. A. Benninghoven *et al.*), pp. 394–397. Chichester: Wiley.

Wittmaack, K. 1996*a* Sputtering yield changes, surface movement and apparent profile shifts in SIMS depth analyses of silicon using oxygen primary ions. *Surf. Interface Analysis* **24**, 389–398.

Wittmaack, K. 1996*b* Angular dependence of sputtering yields and broadening of Ge distributions in Si using oxygen primary ions at different energies. (In preparation.)

Wittmaack, K. & Poker, D. B. 1990 Interface broadening in sputter profiling through alternating layers of isotopically purified silicon. *Nucl. Instrum. Meth.* B **47**, 224–235.

Wittmaack, K. & Wach, W. 1981 Profile distortions and atomic mixing in SIMS analysis using oxygen primary ions. *Nucl. Instrum. Meth.* **191**, 327–334.

Yu, M. L. 1991 Charged and excited states of sputtered atoms. In *Sputtering by particle bombardment III* (ed. R. Behrisch & K. Wittmaack), pp. 91–160. Berlin: Springer.

PHILOSOPHICAL TRANSACTIONS OF THE ROYAL SOCIETY A MATHEMATICAL, PHYSICAL & ENGINEERING SCIENCES

Zalm, P. C., Vriezema, C. J., Gravesteijn, D. J., van de Walle, G. F. A & de Boer, W. B. 1991 Facts and artefacts in the characterization of Si–SiGe multilayers with SIMS. *Surf. Interface Analysis* **17**, 556–566.

Ziegler, J. F., Biersack, J. P. & Littmark, U. 1985 *The stopping and range of ions in solids*, vol. 1. New York: Pergamon.

Discussion

I. W. Drummond (*Kratos Analytical Ltd, UK*). The data presented have dealt almost exclusively, as far as I can tell, on the effects of bombarding silicon (Si) with O_2^+ ions. What is, or what do you feel will be, the effect (if any) on the altered surface layer when Si is bombarded with other oxygen ion species such as O^+ and O^-.

K. Wittmack. As far as one can tell from the limited number of literature data for O^+ and O^- bombardment of Si, the transition fluence, the oxide thickness and the evolution of crater depth versus fluence are essentially the same for O^+ and O_2^+ primary ion beams, provided the results are compared at the same energy per projectile atom (Wittmaack 1996*a*). Even for O^- primary ions (Vriezema & Zalm 1991) the apparent boron profile shift reported for 14.5 keV bombardment at 24°, would fit well into figure 19*a* at an equivalent O_2^+ energy of 29 keV (24° is close to or slightly below the critical angle for SiO_2 formation at this energy).

Additional references

Vriezema, C. J. & Zalm, P. C. 1991 Impurity migration during SIMS depth profiling. *Surf. Interface Analysis* **17**, 875–887.